Coherent optical transient study of molecular collisions: Theory and observations

Paul R. Berman*
Physics Department, New York University, New York, New York 10003

J. M. Levy† and Richard G. Brewer†
IBM Research Laboratory, San Jose, California 95193

(Received 24 October 1974)

It has been shown recently that molecular gas samples excited with coherent light can display a variety of transient phenomena, similar to those found in nuclear magnetic resonance. This article elucidates how these coherence effects can be used to isolate or unfold molecular collision mechanisms that normally remain hidden within the optical line shape. Elastic collisions, for example, are easily detected here in *two-pulse photon echo* experiments for a $^{13}CH_3F$ vibration-rotation transition. The echo-decay function which provides a signature for the velocity-changing collision diffusion mechanism, is not just a simple exponential in time but exhibits an $\exp(-Kt^3)$ contribution for short times and an $\exp(-\Gamma t)$ decay for long times. This behavior, which is unknown heretofore, contrasts with spin echoes in molecular liquids where Brownian motion leads only to the cubic decay law. An $\exp(-Kt^3)$ behavior can be understood in terms of a solution of the Fokker-Planck equation which describes the effect of Brownian motion on echo decay. Such a treatment is valid for small phase excursions; in the case of a gas, this implies the Doppler phase factor $k\Delta u\tau \ll 1$, where $\vec{k}$ is the propagation vector of light, Δu is a characteristic velocity jump for a binary collision, and τ is the echo-pulse delay time. When $k\Delta u\tau \gg 1$ as in the long-time regime, the Fokker-Planck solution fails. We, therefore, present a new solution to the Boltzmann transport equation using a weak collision model and find agreement with the entire echo time dependence observed. The echo measurements indicate very small changes in longitudinal velocity per $^{13}CH_3F$-$^{13}CH_3F$ collision, i.e., $\Delta u = 85$ cm/sec, thereby justifying the weak-collision model. The total elastic collision cross section is 430 Å^2. It follows that elastic collisions lead to velocity thermalization in a time of ~ 5 sec when the $^{13}CH_3F$ pressure is 1 mTorr. A comparison is also made of the $^{13}CH_3F$ dephasing time τ_2 in a *coherent Raman beat* decay, which is independent of velocity-changing collisions, with the longitudinal decay time T_1. Here, T_1 represents the molecule-optical interaction time, due largely to jumps in molecular rotation (J) and orientation (M) state, and is obtained from a *delayed nutation* measurement. The fact that the pressure dependent part of $\tau_2 = T_1$ shows that T_1 is also independent of velocity diffusion. Futhermore, when a hole is burned in the Doppler distribution, population recovery must be due to inelastic rather than elastic collisions. *Optical Carr-Purcell echoes*, multiple pulse echoes, provide a direct measure of the $^{13}CH_3F$ transverse dephasing time T_2 without the effect of elastic collisions while being sensitive to "phase interrupting collisions." Again, we find that $T_2 = T_1$ so that phase interruptions are negligible. Had such a process dominated the two-pulse echo, an $\exp(-t/T_2)$ damping would have been noticed with no $\exp(-Kt^3)$ contribution. Thus, the present study covers several new aspects of molecular collisions. It represents the first detailed examination of velocity-changing collisions by coherence methods and without the complication of Doppler broadening.

I. INTRODUCTION

The role of atomic and molecular collisions in optical line broadening was first demonstrated by Michelson in 1895.[1] Other methods for studying collision phenomena have evolved since, such as molecular-beam[2] and microwave spectroscopy,[3] but in the optical region, Michelson's spectroscopic technique persists even today. This article discusses another optical method, coherent transients, now possible with the availability of laser light and the recently-introduced technique of Stark switching.[4] It has been demonstrated already that molecular samples excited with coherent light over macroscopic dimensions can exhibit a variety of transient phenomena[4-10] that are reminiscent of spin transients in nuclear magnetic resonance (NMR).[11-15] In this way, specific relaxation processes can be isolated in contrast to steady-state optical linewidth measurements which represent a summation over all collision mechanisms. The present work extends a preliminary Letter[8] on this subject and includes details of new theory and experiments.

We shall focus on the translational Brownian motion problem of a dilute molecular gas, $^{13}CH_3F$, and its effect on photon-echo experiments. The measurement described in IV is sensitive to elastic collisions between molecular pairs where the quantum states remain fixed and the linear velocity exhibits a diffusive character through small-angle scattering. The transition frequency of the ra-

diating sample is no longer pure therefore, but displays a bandwidth corresponding to the velocity spread produced by elastic collisions. The various velocity packets diverge in their phase relationship causing the echo amplitude to diminish with a characteristic time dependence that distinguishes the velocity-diffusion mechanism from other dephasing processes. We note that spectral diffusion was not recognized in the echo study of Ref. 4.

The effect of spectral diffusion on optical echoes produced in a molecular gas contrasts markedly with that of spin echoes in a molecular liquid. In the NMR case,[11] a single decay law of the form $\exp(-Kt^3)$ is observed and can be explained by a solution of the Fokker-Planck equation.[16] In the optical case, we observe two limiting time regimes—$\exp(-Kt^3)$ for short times and $\exp(-\Gamma t)$ for long times. We show in Sec. II that for the optical-echo problem, the Fokker-Planck solution fails and the entire time dependence, which is unknown heretofore, can be derived from a solution of the Boltzmann transport equation assuming a weak-collision kernel. The experiments and theory to be presented thus extend our understanding of optical-echo formation in gases and the collision parameters obtained characterize the persistence of molecular velocity in gas samples.

The echo experiments of $^{13}CH_3F$ indicate that the linewidth contribution from velocity-changing collisions is indeed quite small ($\lesssim$0.1 MHz) compared to the Doppler width (~100 MHz) and would be easily masked in a steady-state linewidth measurement. Even certain laser methods, such as Lamb-dip or double resonance, that remove Doppler broadening appear inadequate.[17] An exception is the time-delayed probing of the Lamb-dip linewidth.[18] On the other hand, elastic collisions have a profound influence on the optical phase memory of coherently prepared samples in echo measurements. This makes possible a determination of the characteristic velocity jump, essentially the rms change in velocity per collision, which is found to be only ~0.2% of thermal velocity for $^{13}CH_3F$.

A byproduct of these studies answers the question: Are phase-interrupting collisions important? Quantum mechanical considerations[19,20] of this topic indicate that if the collision interaction is strongly state dependent, the velocity-changing collision contribution to the line shape disappears and the phase-interruption part dominates. On the other hand, if the collision is state independent, it follows that the phase-interruption vanishes and the concept of a velocity-changing collision has meaning. When both contributions are comparable, the theoretical complexity increases considerably. For the vibration-rotation transition of $^{13}CH_3F$ described here, we show that phase interruptions are immeasurably small compared to velocity changes. The conclusion follows from the comparison made in Sec. III of the longitudinal decay time T_1 with that of T_2 from multiple-pulse photon echoes (Carr-Purcell echoes[13]).

II. THEORY

A few theories of echo formation in gases can be found in the literature.[21] In general, the Bloch equations are used to derive an expression for the echo amplitude that will account for simple relaxation processes (i.e., T_1 and T_2 decay), but will not include the effects of collision-induced changes in the velocity of the radiating molecules. Modification of the results to include velocity-changing collisions has been carried out in some cases,[21] but the solutions are based on inappropriate models and do not predict the time dependence discussed here. Therefore, we shall present a simple, but fundamental, solution of the echo problem that is easily extended to the most general case. The calculation will involve (A) a brief review of the physics of echo formation, (B) derivation of formal expressions for the echo-field amplitude in terms of the polarization of the sample, and for the polarization of the sample in terms of density-matrix elements, (C) writing appropriate equations of motion for the density-matrix elements and connecting these with the Bloch equations, (D) solution of the equations and calculation of the echo amplitude in a simplified limit that serves to illustrate the physics, (E) modification of these simplified results for the actual experimental situation, and (F) an interpretation of the results. Approximations and assumptions of our model will be explicitly stated throughout.

A. Echo formation

To produce photon echoes in a molecular gas, one first subjects the sample to a radiation pulse that produces an array of dipoles that are initially in phase. These dipoles radiate and begin to dephase owing to their motion. The relative dephasing of a molecule moving with velocity $\vec{v}$ will be $\vec{k}\cdot\vec{v}t$ where $\vec{k}$ is the radiation propagation vector and t the time elapsed after the applied pulse.

Another pulse applied to the sample at time τ (see Fig. 1) can produce a phase change of $-2\vec{k}\cdot\vec{v}\tau$ in molecules moving with velocity $\vec{v}$ so that the relative phase of such molecules at time τ will be $\vec{k}\cdot\vec{v}\tau - 2\vec{k}\cdot\vec{v}\tau = -\vec{k}\cdot\vec{v}\tau$. Since the phase of each molecule still increases an amount $\vec{k}\cdot\vec{v}\Delta t$ in a time Δt, one easily sees that at time $t=2\tau$ the molecules are all in phase once again and an "echo" pulse is emitted. The photon-echo amplitude will

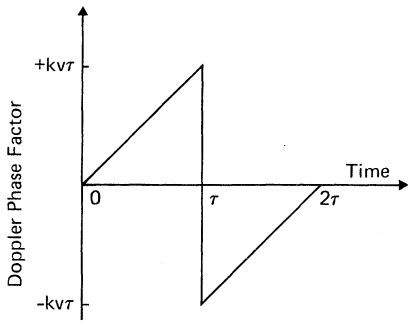

FIG. 1. Relative Doppler phase of molecules with axial velocity $\vec{v}$ is shown. The molecules are all in phase because of a $\frac{1}{2}\pi$ pulse at $t=0$. The phase then advances but reverses sign at $t=\tau$ by application of the π pulse. At $t=2\tau$, the molecular dipoles have all rephased again and an echo signal is produced.

serve to monitor all relaxation processes that interfere with this dephasing-rephasing cycle and is a sensitive probe of collision effects in gases.

B. Polarization and field equations

As long as the echo-field amplitude is much less than the laser-field amplitude and the pulse duration is much greater than an inverse optical cycle, a rather simple expression for the echo amplitude in terms of the medium's polarization can be obtained. The wave equation in a lossless medium for the electric-field amplitude $E(z,t)$ of a wave polarized in the x direction and propagating in the z direction with negligible transverse spatial variation is

$$\frac{\partial^2 E(z,t)}{\partial z^2} - \frac{1}{c^2}\frac{\partial^2 E(z,t)}{\partial t^2} = \frac{4\pi}{c^2}\frac{\partial^2 P(z,t)}{\partial t^2}, \tag{1}$$

where $P(z,t)$ is the x component of the medium's polarization.

The calculation involves a quantum mechanical evaluation of the polarization of the medium induced by the laser field followed by a determination of the corresponding echo-field amplitude from Eq. (1). A consistent solution can be obtained by assuming that a laser field of the form

$$E_L(z,t) = E_0 \cos(kz - \omega_L t) \tag{2}$$

with oscillation frequency ω_L and propagation vector $\vec{k} = k\hat{z}$ will give rise to a polarization

$$P(z,t) = C(t)\cos(kz - \omega_L t) + S(t)\sin(kz - \omega_L t), \tag{3}$$

and, in turn, to an echo field

$$E(z,t) = E_C(z,t)\cos(kz - \omega_L t) + E_S(z,t)\sin(kz - \omega_L t), \tag{4}$$

where $C(t)$, $S(t)$, $E_C(z,t)$, and $E_S(z,t)$ are slowly varying functions of z and t compared with $\sin(kz)$ and $\sin(\omega_L t)$, respectively. Substituting (3) and (4) into (1) and keeping only lowest order terms, yields amplitude equations

$$\left(\frac{\partial}{\partial z} + \frac{1}{c}\frac{\partial}{\partial t}\right)E_C(z,t) = -\frac{2\pi\omega_L}{c}S(t), \tag{5a}$$

$$\left(\frac{\partial}{\partial z} + \frac{1}{c}\frac{\partial}{\partial t}\right)E_S(z,t) = \frac{2\pi\omega_L}{c}C(t). \tag{5b}$$

To calculate C and S, we must calculate the polarization induced by the laser field. The system is assumed to consist of nondegenerate two-level molecules with upper state a and lower state b separated by frequency ω. The polarization of this molecular system is given simply by the sum of expectation values of the dipole-moment operators for each molecule, i.e.,

$$\vec{P}(\vec{R},t) = \int \sum_j e\langle \vec{r}_j\rangle \delta(\vec{R}_j - \vec{R})\, d^3R_j, \tag{6}$$

where $\vec{r}_j$ is the relative electronic coordinate of molecule j, $\vec{R}_j$ is the center-of-mass coordinate of molecule j, the sum is over all molecules, and we have taken a one-electron system without loss of generality. Note that $\langle \vec{r}_j\rangle$ is a function of $\vec{R}_j$ and t since the wave function for the two-level jth molecule is

$$\psi^j(\vec{r}_j, \vec{R}_j, t) = A_a^j(\vec{R}_j, t)\psi_a(\vec{r}_j) + A_b^j(\vec{R}_j, t)\psi_b(\vec{r}_j), \tag{7}$$

where $\psi_a(\vec{r}_j)$ and $\psi_b(\vec{r}_j)$ are molecular-state eigenfunctions and $A_a^j(\vec{R}_j, t)$ and $A_b^j(\vec{R}_j, t)$ are probability amplitudes. Using Eqs. (6) and (7) and parity considerations, one easily calculates

$$\vec{P}(\vec{R},t) = e\vec{r}_{ab}\rho_{ba}(\vec{R},t) + \text{c.c.}, \tag{8}$$

where

$$\vec{r}_{ab} = \int \psi_a^*(\vec{r})\,\vec{r}\,\psi_b(\vec{r})\, d^3r, \tag{9}$$

c.c. stands for complex conjugate, and

$$\rho_{\alpha\alpha'}(\vec{R},t) = \sum_j A_\alpha^j(\vec{R},t)A_{\alpha'}^j(\vec{R},t)^* \tag{10}$$

is the $\alpha\alpha'$ density-matrix element. Rather than deal with the purely quantum mechanical density-matrix elements $\rho_{\alpha\alpha'}(\vec{R},t)$, it is possible to go over to density-matrix elements in classical phase space $\rho_{\alpha\alpha'}(\vec{R},\vec{v},t)$ which obey a structurally simple transport equation to be given below. In terms of the $\rho_{\alpha\alpha'}(\vec{R},\vec{v},t)$ which are functions of the classical position and velocity variables $\vec{R}$ and $\vec{v}$ respectively [$\rho_{\alpha\alpha'}(\vec{R},t)$ was a function of the quantum mechanical variable $\vec{R}$] the x component of polarization is simply

$$P(\vec{R},t) = \int d^3v\,[ex_{ba}\rho_{ab}(\vec{R},\vec{v},t) + \text{c.c.}]. \tag{11}$$

Thus, one must (a) solve a transport equation (to be given) to obtain $\rho_{ab}(\vec{R}, \vec{v}, t)$, (b) calculate $P(\vec{R}, t)$ using (11), (c) write $P(\vec{R}, t)$ in the form of Eq. (3) to determine $C(t)$ and $S(t)$, and (d) finally, obtain the echo field amplitudes $E_S(z, t)$ and $E_C(z, t)$ from a solution of Eq. (5). Note that, experimentally, we measure the time-averaged quantity

$$I \propto \langle |E_L(z, t) + E(z, t)|^2 \rangle \approx \tfrac{1}{2}E_0^2 + E_C(z, t)E_0, \quad (12)$$

where terms of order E_C^2 have been dropped. Thus, in the experiments to be discussed, the echo signal $E_C(z, t)E_0$ appears as a heterodyne beat superimposed on a dc signal $\frac{1}{2}E_0^2$.

C. Density matrix and Bloch equations

The density-matrix elements $\rho_{\alpha\alpha'}(\vec{R}, \vec{v}, t)$ obey a quantum mechanical transport equation that consistently takes into account the interaction of the molecular system with external fields while collisions are occurring within the system.[20] The equation appropriate for the experimental situation is

$$\begin{aligned}\frac{\partial \rho_{\alpha\alpha'}(\vec{R},\vec{v},t)}{\partial t} &= -\vec{v}\cdot\vec{\nabla}\rho_{\alpha\alpha'}(\vec{R},\vec{v},t) \\ &+ (i\hbar)^{-1}[H_0 + V(\vec{R},t), \rho(\vec{R},\vec{v},t)]_{\alpha\alpha'} \\ &- (1/T_1)\rho_{\alpha\alpha'}(\vec{R},\vec{v},t) - \Gamma\rho_{\alpha\alpha'}(\vec{R},\vec{v},t) \\ &+ \int d^3v'\, W(\vec{v}'\to\vec{v})\rho_{\alpha\alpha'}(\vec{R},\vec{v}',t).\end{aligned} \quad (13)$$

The contributions to $\partial\rho_{\alpha\alpha'}(\vec{R}, \vec{v}, t)/\partial t$ are (a) a convective flow term $-\vec{v}\cdot\vec{\nabla}\rho_{\alpha\alpha'}(\vec{R}, \vec{v}, t)$, (b) the change in $\rho_{\alpha\alpha'}$ due to the free molecular Hamiltonian H_0,

$$(i\hbar)^{-1}[H_0, \rho(\vec{R},\vec{v},t)]_{\alpha\alpha'} = -i\omega_{\alpha\alpha'}\rho_{\alpha\alpha'}(\vec{R},\vec{v},t), \quad (14)$$

with

$$\omega_{\alpha\alpha'} = (E_\alpha - E_{\alpha'})/\hbar, \quad (15)$$

and E_α the free-molecule eigenenergy of state α, (c) the change in $\rho'_{\alpha\alpha}$ due to the molecule-optical-field interaction

$$(i\hbar)^{-1}[V(\vec{R}, t), \rho(\vec{R}, \vec{v}, t)]_{\alpha\alpha'},$$

with matrix elements of $V(\vec{R}, t)$ given by

$$V_{\alpha\alpha'}(\vec{R}, t) = -ex_{\alpha\alpha'}E_L(\vec{R}, t), \quad (16)$$

in which $E_L(\vec{R}, t)$ is the laser field [Eq. (2)], and the effect on the sample due to the echo field has been assumed negligible, (d) a *population* loss term $-(1/T_1)\rho_{\alpha\alpha'}(\vec{R}, \vec{v}, t)$ due to effects such as quenching collisions and molecular transit out of the laser beam with T_1^{-1} being the rate for such processes (an assumption implicit in writing such a term is that population losses are state independent which is reasonable for different vibrational levels of a given electronic state), (e) a term $-\Gamma\rho_{\alpha\alpha'}(\vec{R}, \vec{v}, t)$ giving the loss of $\rho_{\alpha\alpha'}(\vec{R},\vec{v},t)$ due to velocity-changing collisions occurring with rate Γ, and (f) a term

$$\int d^3v'\, W(\vec{v}'\to\vec{v})\rho_{\alpha\alpha'}(\vec{R}, \vec{v}', t)$$

giving an increase in $\rho_{\alpha\alpha'}(\vec{R}, \vec{v}, t)$ due to velocity-changing collisions associated with the collision kernel $W(\vec{v}'\to\vec{v})$ that bring molecules from velocity $\vec{v}'$ to $\vec{v}$.

The fact that both Γ and $W(\vec{v}'\to\vec{v})$ are real $[\Gamma = \int d^3v'\, W(\vec{v}\to\vec{v}')]$, is a consequence of the assumption that the collision interaction is state independent—the only effect of a collision is to change the velocity of the molecule. Furthermore, (13) implies that $T_2 = T_1$ because phase-interrupting collisions are assumed negligible. In the more general case of a state-dependent collision interaction, additional terms would be needed in the transport equation[20] and then $T_2 \neq T_1$. Furthermore, for simplicity we have assumed T_1 and Γ to be independent of molecular speed v—allowance for the speed dependence of these variables would not significantly affect any of the results.[22] Finally, we should note that pumping terms are excluded from (13) on the assumption that any molecules pumped into the lower state after the initial laser pulse will not contribute to the echo amplitude.

In terms of components for our two-level system with $V(\vec{R}, t)$ given by (16) and $E_L(\vec{R}, t)$ given by (2), Eq. (13) becomes

$$(\partial/\partial t + \vec{v}\cdot\vec{\nabla})\rho_{aa}(\vec{R},\vec{v},t) = -i\chi\cos(kz - \omega_L t)[\rho_{ab}(\vec{R},\vec{v},t) - \rho_{ba}(\vec{R},\vec{v},t)] - (\Gamma_1 + \Gamma)\rho_{aa}(\vec{R},\vec{v},t) + \int d^3v'\, W(\vec{v}'\to\vec{v})\rho_{aa}(\vec{R},\vec{v}',t), \quad (17a)$$

$$(\partial/\partial t + \vec{v}\cdot\vec{\nabla})\rho_{ab}(\vec{R},\vec{v},t) = -i\omega\rho_{ab}(\vec{R},\vec{v},t) - i\chi\cos(kz - \omega_L t)[\rho_{aa}(\vec{R},\vec{v},t) - \rho_{bb}(\vec{R},\vec{v},t)] - (\Gamma_1 + \Gamma)\rho_{ab}(\vec{R},\vec{v},t) + \int d^3v'\, W(\vec{v}'\to\vec{v})\rho_{ab}(\vec{R},\vec{v}',t), \quad (17b)$$

where

$$\Gamma_1 = (T_1)^{-1}, \quad (18)$$

$$\chi = ex_{ab}E_0/\hbar, \quad (19)$$

$$\omega = \omega_a - \omega_b, \quad (20)$$

x_{ab} is taken as real, and equations for ρ_{bb} and ρ_{ba} can be obtained by interchanging a and b (and ω with $-\omega$) in the above equations. The normalization taken for ρ is

$$\sum_{\alpha}\int \rho_{\alpha\alpha}(\vec{R},\vec{v},t)\,d^3R\,d^3v = \mathfrak{N},$$

where $\mathfrak{N}$ is the total number of active molecules.

By writing

$$\rho_{ab}(\vec{R},\vec{v},t) = \tilde{\rho}_{ab}(\vec{R},\vec{v},t)\exp i(\vec{k}\cdot\vec{R}-\omega_L t), \tag{21}$$

with $\vec{k}=k\hat{z}$ and $\tilde{\rho}_{ab}(\vec{R},\vec{v},t)$ assumed to be slowly varying in space compared with $\cos(kz)$ and in time compared with $\cos(\omega_L t)$ and by using the rotating-wave approximation [neglect of rapidly varying terms in Eqs. (17)], Eqs. (17) can be reduced to

$$(\partial/\partial t+\vec{v}\cdot\vec{\nabla})\rho_{aa}(\vec{R},\vec{v},t) = -i(\tfrac{1}{2}\chi)[\tilde{\rho}_{ab}(\vec{R},\vec{v},t)-\tilde{\rho}_{ba}(\vec{R},\vec{v},t)] - (\Gamma_1+\Gamma)\rho_{aa}(\vec{R},\vec{v},t) + \int d^3v'\,W(\vec{v}'\to\vec{v})\rho_{aa}(\vec{R},\vec{v}',t), \tag{22a}$$

$$(\partial/\partial t+\vec{v}\cdot\vec{\nabla})\tilde{\rho}_{ab}(\vec{R},\vec{v},t) = -i(\omega-\omega_L+\vec{k}\cdot\vec{v})\tilde{\rho}_{ab}(\vec{R},\vec{v},t) - i(\tfrac{1}{2}\chi)[\rho_{aa}(\vec{R},\vec{v},t)-\rho_{bb}(\vec{R},\vec{v},t)] - (\Gamma_1+\Gamma)\tilde{\rho}_{ab}(\vec{R},\vec{v},t) + \int d^3v'\,W(\vec{v}'\to\vec{v})\tilde{\rho}_{ab}(\vec{R},\vec{v}',t), \tag{22b}$$

plus equations with $a\rightleftharpoons b$ and $(\omega-\omega_L+\vec{k}\cdot\vec{v}) \rightleftharpoons -(\omega-\omega_L+\vec{k}\cdot\vec{v})$.

Equations (22) are the starting point for the theoretical calculations. Some authors prefer to use linear combinations of density-matrix elements. For example, defining

$$m(\vec{R},\vec{v},t) = \rho_{aa}(\vec{R},\vec{v},t)+\rho_{bb}(\vec{R},\vec{v},t), \tag{23a}$$

$$w(\vec{R},\vec{v},t) = \rho_{aa}(\vec{R},\vec{v},t)-\rho_{bb}(\vec{R},\vec{v},t), \tag{23b}$$

$$v(\vec{R},\vec{v},t) = i[\tilde{\rho}_{ab}(\vec{R},\vec{v},t)-\tilde{\rho}_{ba}(\vec{R},\vec{v},t)], \tag{23c}$$

$$u(\vec{R},\vec{v},t) = \tilde{\rho}_{ab}(\vec{R},\vec{v},t)+\tilde{\rho}_{ba}(\vec{R},\vec{v},t), \tag{23d}$$

[the variable $v(\vec{R},\vec{v},t)$ is to be distinguished from the velocity $\vec{v}$], one can transform Eqs. (22) into

$$(\partial/\partial t+\vec{v}\cdot\vec{\nabla})m(\vec{R},\vec{v},t) = -(\Gamma_1+\Gamma)m(\vec{R},\vec{v},t) + \int d^3v'\,W(\vec{v}'\to\vec{v})m(\vec{R},\vec{v}',t) \tag{24a}$$

$$(\partial/\partial t+\vec{v}\cdot\vec{\nabla})w(\vec{R},\vec{v},t) = -(\Gamma_1+\Gamma)w(\vec{R},\vec{v},t) + \int d^3v'\,W(\vec{v}'\to\vec{v})w(\vec{R},\vec{v}',t) - \chi v(\vec{R},\vec{v},t), \tag{24b}$$

$$(\partial/\partial t+\vec{v}\cdot\vec{\nabla})v(\vec{R},\vec{v},t) = -(\Gamma_1+\Gamma)v(\vec{R},\vec{v},t) + \int d^3v'\,W(\vec{v}'\to\vec{v})v(\vec{R},\vec{v}',t) + (\omega-\omega_L+\vec{k}\cdot\vec{v})u(\vec{R},\vec{v},t) + \chi w(\vec{R},\vec{v},t), \tag{24c}$$

$$(\partial/\partial t+\vec{v}\cdot\vec{\nabla})u(\vec{R},\vec{v},t) = -(\Gamma_1+\Gamma)u(\vec{R},\vec{v},t) + \int d^3v'\,W(\vec{v}'\to\vec{v})u(\vec{R},\vec{v},t) - (\omega-\omega_L+\vec{k}\cdot\vec{v})v(\vec{R},\vec{v},t). \tag{24d}$$

More compactly, we can define a quantity

$$\delta(\omega) = (\omega-\omega_L+\vec{k}\cdot\vec{v}), \tag{25}$$

and vectors

$$\vec{B}(\vec{R},\vec{v},t) \equiv (u(\vec{R},\vec{v},t), v(\vec{R},\vec{v},t), w(\vec{R},\vec{v},t)) \tag{26}$$

and

$$\vec{\Omega} = (-\chi, 0, \delta(\omega)), \tag{27}$$

enabling one to write Eqs. (24b)–(24d) as

$$(\partial/\partial t+\vec{v}\cdot\vec{\nabla})\vec{B}(\vec{R},\vec{v},t) = \vec{\Omega}\times\vec{B}(\vec{R},\vec{v},t) - (\Gamma_1+\Gamma)\vec{B}(\vec{R},\vec{v},t) + \int d^3v'\,W(\vec{v}'\to\vec{v})\vec{B}(\vec{R},\vec{v}',t), \tag{28}$$

which is just a generalized form of the Bloch equations equivalent to Eq. (22) for density-matrix elements.

The assumption is made that the laser beam is uniform over a homogeneous sample which implies that any spatial variation of the vector variable $\vec{B}(\vec{R},\vec{v},t)$ is to be neglected so that its $\vec{R}$ argument can be dropped. Furthermore a new vector variable

$$\vec{B}'(\vec{v},t) = (u'(\vec{v},t), v'(\vec{v},t), w'(\vec{v},t)) = \vec{B}(\vec{v},t)e^{\Gamma_1 t}, \tag{29}$$

can be used to transform Eq. (28) into

$$\frac{\partial\vec{B}'(\vec{v},t)}{\partial t} = \vec{\Omega}\times\vec{B}'(\vec{v},t) - \Gamma\vec{B}'(\vec{v},t) + \int d^3v'\,W(\vec{v}'\to\vec{v})\vec{B}'(\vec{v}',t). \tag{30}$$

The initial condition at $t=0$, assuming the molecules are in their ground state is

$$\vec{B}'(\vec{v},0) = (0, 0, -NW_0(\vec{v})), \tag{31}$$

where $W_0(\vec{v})$ is the normalized thermal equilibrium initial molecular-velocity distribution and N is the density of active molecules.

D. Solution of the equations - echo amplitude

Equations (22) or (30) may now be solved for our experimental situation in which the laser field is always present and the molecular transition is switched in or out of resonance by application of a Stark field. The molecular transition frequency shall be designated by ω_0 with the Stark field off and ω_s with it on. The pulse sequence is shown in Fig. 2.

From $t=0$ to $t=t_1$ and from $t=t_2$ to $t=t_3$, $\omega=\omega_s$ and at all other times the Stark field is off so that $\omega=\omega_0$. The molecules start in their ground state at $t=0$ and the first pulse excites them into a linear superposition state. The time t_1 is assumed short enough to neglect all relaxation processes in this interval. From $t=t_1$ to $t=t_2$, $\omega=\omega_0$ and the molecules of concern are so far off resonance that, for all practical purposes, we can effectively take $\chi\equiv 0$ in Eqs. (24) for this time region. During this interval, the molecules will dephase due to their Doppler motion, emitting a free-induction-decay[7] signal. Collisions and other relaxation processes are also taken into account. From $t=t_2$ to $t=t_3$, the molecules are switched back into near resonance with the field and this pulse will produce a phase change in some of the molecules that will start them rephasing. All relaxation processes are neglected in the $t_2 \rightarrow t_3$ interval. Finally, from $t=t_3$ to the observation time t, $\omega=\omega_0$ and we again can effectively take $\chi\equiv 0$. Those molecules, which have been properly rephased by the second pulse, will produce a maximum echo signal when $t-t_3 = t_2-t_1$ unless collisions or other relaxation processes have come into play.

To carry out the calculation, a choice for the collision kernel $W(\vec{v}'\rightarrow\vec{v})$ must be made. *Since the functional dependence of the results will be independent of the choice of kernel,* we have adopted the Brownian motion kernel of Keilson and Storer,[23]

$$W(\vec{v}'\rightarrow\vec{v}) = \Gamma(\pi\Delta u^2)^{-3/2}\exp[-(\vec{v}-\alpha\vec{v}')^2/\Delta u^2], \quad (32)$$

where Γ is the (speed independent) rate of elastic collisions, α is a constant close to unity, and Δu, determined by

$$\Delta u^2 = (1-\alpha^2)u^2 \approx 2(1-\alpha)u^2, \quad (33)$$

is root two times the rms change in velocity per collision while u is the most probable speed of the *thermal equilibrium* distribution. Equation (33) follows from imposing detailed balancing, Eq. (40). The kernel (32) is mathematically simple to deal with and the assumption that $\alpha\approx 1$, which corresponds to having very small changes in velocity per collision, will be supported by the experimental data. Definitions of variables to be used in the calculation appear in Table I in Appendix A.

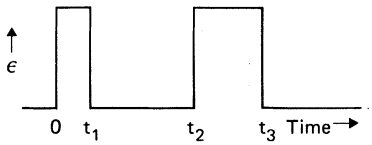

FIG. 2. Pulse sequence showing the Stark field amplitude ϵ versus time. The two pulses occur over the intervals $t=0$ to t_1, and $t=t_2$ to t_3.

Simplified case

In order to illustrate the physics of the problem, we first consider a simplified case in which the time intervals t_1 and t_3-t_2 are assumed so short that $|\delta(\omega_s)t_1|\ll 1$ and $|\delta(\omega_s)(t_3-t_2)|\ll 1$ for all molecules of the sample while at the same time the optical-field strength is large enough so that $\chi t_1\approx 1$ and $\chi(t_3-t_2)\approx 1$. Physically, this corresponds to assuming that the pulses uniformly excite the entire thermal distribution of molecules. In this model, collisions change the velocity (and, consequently the phase) of *individual* molecules but do not alter the velocity *distribution* of the ensemble. Modifications of the theory to account for the actual experimental situation in which only a fraction of the bandwidth is excited by the pulses will be discussed below.

The solution is now traced for each time region shown in Fig. 2.

a. $0<t<t_1$. In component form, Eq. (30) becomes

$$\dot{u}'(\vec{v},t)=0, \quad (34a)$$

$$\dot{v}'(\vec{v},t)=\chi w'(\vec{v},t), \quad (34b)$$

$$\dot{w}'(\vec{v},t)=-\chi v'(\vec{v},t), \quad (34c)$$

having used the fact that $\Gamma t_1\ll 1$ and $|\delta(\omega_s)|t_1\ll 1$. The solution of Eqs. (34) at $t=t_1$ subject to initial condition (31) is

$$u'(\vec{v},t_1)=0, \quad (35a)$$

$$v'(\vec{v},t_1)=-NW_0(\vec{v})\sin\chi t_1, \quad (35b)$$

$$w'(\vec{v},t_1)=-NW_0(\vec{v})\cos\chi t_1. \quad (35c)$$

We can further simplify matters by choosing t_1 such that $\chi t_1=\frac{1}{2}\pi$ leading to

$$v'(\vec{v},t_1)=-NW_0(\vec{v}), \quad w'(\vec{v},t_1)=u'(\vec{v},t_1)=0. \quad (36)$$

b. $t_1<t<t_2$. In this region $\omega=\omega_0$ and χ is effectively zero giving a value of $\vec{\Omega}$ equal to

$$\vec{\Omega}_0=(0,0,\delta(\omega_0)), \quad (37)$$

to be used in Eq. (30). A trial solution of the form

$$\vec{B}'(\vec{v},t)=NW_0(\vec{v})\vec{\tilde{B}}'(\vec{v},t)$$
$$=NW_0(\vec{v})[\tilde{u}'(\vec{v},t),\tilde{v}'(\vec{v},t),\tilde{w}'(\vec{v},t)], \quad (38)$$

when substituted in Eq. (30) yields

$$W_0(\vec{v})\dot{\vec{\tilde{B}}}'(\vec{v},t)=W_0(\vec{v})\vec{\Omega}_0\times\vec{B}'(\vec{v},t)-W_0(\vec{v})\Gamma\vec{\tilde{B}}'(\vec{v},t)$$
$$+\int d^3v'\,W(\vec{v}'\to\vec{v})W_0(\vec{v}')\vec{\tilde{B}}'(\vec{v}',t). \quad (39)$$

Since $W_0(\vec{v}')$ is the thermal-equilibrium distribution, detailed balancing requires

$$W(\vec{v}'\to\vec{v})W_0(\vec{v}')=W_0(\vec{v})W(\vec{v}\to\vec{v}'), \quad (40)$$

and $W_0(\vec{v})$ may be factored from Eq. (39) leaving

$$\dot{\vec{\tilde{B}}}'(\vec{v},t)=\vec{\Omega}_0\times\vec{\tilde{B}}'(\vec{v},t)-\Gamma\vec{\tilde{B}}'(\vec{v},t)$$
$$+\int d^3v'\,W(\vec{v}\to\vec{v}')\vec{\tilde{B}}'(\vec{v}',t), \quad (41)$$

subject to the initial condition [obtained from Eqs. (36) and (38)]

$$\vec{\tilde{B}}'(\vec{v},\vec{t}_1)=[0,-1,0]. \quad (42)$$

In terms of components, Eq. (41) is

$$\dot{\tilde{u}}'(\vec{v},t)=-\delta(\omega_0)\tilde{v}'(\vec{v},t)-\Gamma\tilde{u}'(\vec{v},t)$$
$$+\int d^3v'\,W(\vec{v}\to\vec{v}')\tilde{u}'(\vec{v}',t), \quad (43a)$$

$$\dot{\tilde{v}}'(\vec{v},t)=\delta(\omega_0)\tilde{u}'(\vec{v},t)-\Gamma\tilde{v}'(\vec{v},t)$$
$$+\int d^3v'\,W(\vec{v}\to\vec{v}')\tilde{v}'(\vec{v}',t), \quad (43b)$$

$$\dot{\tilde{w}}'(\vec{v},t)=-\Gamma\tilde{w}'(\vec{v},t)+\int d^3v'\,W(\vec{v}\to\vec{v}')\tilde{w}'(\vec{v}',t). \quad (43c)$$

For the assumed thermal-equilibrium condition, the solution of (43c) is simply

$$\tilde{w}'(\vec{v},t)=\tilde{w}'(\vec{v},t_1),$$

so that, using (36) and (38), one finds

$$w'(\vec{v},t_2)=0. \quad (44)$$

Equations (43a) and (43b) are most easily studied by introducing a variable

$$\tilde{\rho}'_{ab}(\vec{v},t,t_1)=\tfrac{1}{2}\{\exp[i\delta(\omega_0)(t-t_1)]\}[\tilde{u}'(\vec{v},t)-i\tilde{v}'(\vec{v},t)]. \quad (45)$$

Recalling that $\delta(\omega_0)=(\omega_0-\omega_L+\vec{k}\cdot\vec{v})$ and using Eqs. (43a) and (43b), we may show that $\tilde{\rho}'_{ab}$ obeys the equation

$$\frac{\partial\tilde{\rho}'_{ab}(\vec{v},t,t_1)}{\partial t}=-\Gamma\tilde{\rho}'_{ab}(\vec{v},t,t_1)$$
$$+\int d^3v'\,W(\vec{v}\to\vec{v}')$$
$$\times\exp[i\vec{k}\cdot(\vec{v}-\vec{v}')(t-t_1)]\tilde{\rho}'_{ab}(\vec{v}',t,t_1), \quad (46)$$

subject to the initial condition

$$\tilde{\rho}'_{ab}(\vec{v},t_1,t_1)=\tfrac{1}{2}[\tilde{u}'(\vec{v},t_1)-i\tilde{v}'(\vec{v},t_1)]=\tfrac{1}{2}i. \quad (47)$$

We try a solution of the form

$$\tilde{\rho}'_{ab}(\vec{v},t,t_1)=\tfrac{1}{2}i\exp[i\vec{x}(t,t_1)\cdot\vec{v}+y(t,t_1)], \quad (48)$$

where the variables $\vec{x}$ and y satisfy initial conditions

$$\vec{x}(t_1,t_1)=0, \quad y(t_1,t_1)=0. \quad (49)$$

Substituting (48) into (46), one arrives at the equation

$$i\dot{\vec{x}}\cdot\vec{v}+\dot{y}=-\Gamma+\int d^3v'\,W(\vec{v}\to\vec{v}')$$
$$\times\exp\{i[\vec{k}(t-t_1)-\vec{x}]\cdot(\vec{v}-\vec{v}')\}, \quad (50)$$

which, after inserting the explicit kernel $W(\vec{v}\to\vec{v}')$ given by (32) into the integral and performing the $\vec{v}'$ integration, may be reduced to

$$i\dot{\vec{x}}\cdot\vec{v}+\dot{y}=-\Gamma+\Gamma\exp\{i(1-\alpha)[\vec{k}(t-t_1)-\vec{x}]\circ\vec{v}\}$$
$$\times\exp\{-[\vec{k}(t-t_1)-\vec{x}]^2\Delta u^2/4\}. \quad (51)$$

The second term will contribute only if

$$[\vec{k}(t-t_1)-\vec{x}]^2\Delta u^2\lesssim 1 \quad (52)$$

and, in that case [using Eq. (33)], the first exponent

$$|(1-\alpha)[\vec{k}(t-t_1)-\vec{x}]\circ\vec{v}|=|[\vec{k}(t-t_1)-\vec{x}]\cdot\vec{v}\Delta u^2/(2u^2)|$$
$$\lesssim|\vec{k}(t-t_1)-\vec{x}|\Delta u(\Delta u/u)\ll 1$$

enabling one to expand the lead exponential in Eq. (51) to obtain

$$i\dot{\vec{x}}\cdot\vec{v}+\dot{y}\approx-\Gamma+\Gamma(\exp\{-[\vec{k}(t-t_1)-\vec{x}]^2\Delta u^2/4\})$$
$$\times\{1+i(1-\alpha)[\vec{k}(t-t_1)-\vec{x}]\circ\vec{v}\}. \quad (53)$$

This equation immediately yields two equations

$$\dot{\vec{x}}(t,t_1)=\Gamma(1-\alpha)[\vec{k}(t-t_1)-\vec{x}]$$
$$\times\exp\{-[\vec{k}(t-t_1)-\vec{x}]^2\Delta u^2/4\}, \quad (54a)$$

$$\dot{y}(t,t_1)=-\Gamma(1-\exp\{-[\vec{k}(t-t_1)-\vec{x}]^2\Delta u^2/4\}), \quad (54b)$$

which may be numerically integrated to find $x(t,t_1)$ and $y(t,t_1)$. It might be noted that if the exponent in Eqs. (54) is much less than unity, Eqs. (54) reduce to similar equations obtained by solving the echo problem using a Fokker-Planck[11,16,21,24] rather than a transport equation. Thus, the validity condition for the Fokker-Planck treatment is Eq. (52). The physical implications of that equation will be discussed below.

It is possible to find an analytic solution to Eqs. (54) for a case of practical interest. Since echo signals are only observable for pulse separations

τ such that $\Gamma\tau \lesssim 1$ and since $(1-\alpha) \ll 1$, for all t of interest

$$\Gamma(1-\alpha)t = \Gamma t \Delta u^2/2u^2 \ll 1. \tag{55}$$

Equation (55) shows that the time of approach to a thermal-equilibrium velocity distribution $[\Gamma(1-\alpha)]^{-1}$ is orders of magnitude longer than the experimental observation time $1/\Gamma$. To solve Eqs. (54) in this limit, we further assume

$$|\vec{x}| \ll |\vec{k}|(t-t_1), \tag{56}$$

leading to an immediate solution

$$\vec{x}(t,t_1) = 2\Gamma(1-\alpha)\vec{k}(k^2\Delta u^2)^{-1}\{1-\exp[-k^2(t-t_1)^2\Delta u^2/4]\}, \tag{57a}$$

$$y(t,t_1) = -\Gamma(t-t_1) + \frac{2\Gamma}{k\Delta u}\int_0^{k\Delta u(t-t_1)/2} e^{-\eta^2}\,d\eta. \tag{57b}$$

It is easy to verify that (56) is satisfied when (55) holds.

Using Eqs. (48), (45), and (38), one may finally obtain

$$u'(\vec{v},t_2) = (\tfrac{1}{2}i)NW_0(\vec{v})\exp[-i\delta(\omega_0)(t_2-t_1)] \times \exp[i\vec{x}(t_2,t_1)\cdot\vec{v} + y(t_2,t_1)] + \text{c.c.}, \tag{58a}$$

$$v'(\vec{v},t_2) = -\tfrac{1}{2}NW_0(\vec{v})\exp[-i\delta(\omega_0)(t_2-t_1)] \times \exp[i\vec{x}(t_2,t_1)\cdot\vec{v} + y(t_2,t_1)] + \text{c.c.} \tag{58b}$$

c. $t_2 < t < t_3$. Equations (34) are once again applicable and are easily solved to give

$$u'(\vec{v},t_3) = u'(\vec{v},t_2), \tag{59a}$$

$$v'(\vec{v},t_3) = \cos[\chi(t_3-t_2)]\,v'(\vec{v},t_2) + \sin[\chi(t_3-t_2)]\,w'(\vec{v},t_2), \tag{59b}$$

$$w'(\vec{v},t_3) = \cos[\chi(t_3-t_2)]\,w'(\vec{v},t_2) - \sin[\chi(t_3-t_2)]\,v'(\vec{v},t_2), \tag{59c}$$

and to simplify matters we assume that $t_3 - t_2$ is chosen such that $\chi(t_3-t_2) = \pi$ (a π pulse). In that case one finds

$$u'(\vec{v},t_3) = u'(\vec{v},t_2), \tag{60a}$$

$$v'(\vec{v},t_3) = -v'(\vec{v},t_2), \tag{60b}$$

$$w'(\vec{v},t_3) = 0, \tag{60c}$$

where Eq. (44) has been used.

d. $t_3 < t$. We can proceed as in the $t_1 < t < t_2$ region. The quantity

$$w'(\vec{v},t) = 0, \tag{61}$$

and the variable $\tilde{\rho}'_{ab}(\vec{v},t,t_3+t_2-t_1)$ defined by (45) satisfies the differential equation (46) subject to the initial condition

$$\begin{aligned}\tilde{\rho}'_{ab}(\vec{v},t_3,t_3+t_2-t_1) &= \tfrac{1}{2}[NW_0(\vec{v})]^{-1}[u'(\vec{v},t_3) - iv'(\vec{v},t_3)]\exp[-i\delta(\omega_0)(t_2-t_1)]\\ &= \tfrac{1}{2}[NW_0(\vec{v})]^{-1}[u'(\vec{v},t_2) + iv'(\vec{v},t_2)]\exp[-i\delta(\omega_0)(t_2-t_1)]\\ &= \tilde{\rho}'_{ab}(\vec{v},t_2,t_1)^*\\ &= -\tfrac{1}{2}i\exp[-i\vec{x}(t_2,t_1)\cdot\vec{v} + y(t_2,t_1)].\end{aligned} \tag{62}$$

We see that the effect of a π pulse is simply to convert $\tilde{\rho}'_{ab}$ to its complex conjugate. The second time variable is chosen as $(t_3+t_2-t_1)$ in $\tilde{\rho}'_{ab}(\vec{v},t,t_3+t_2-t_1)$ solely for convenience. With this choice, the Doppler phase $\vec{k}\cdot\vec{v}(t_2-t_1)$ has been eliminated from the initial condition (62), and we can solve for $\tilde{\rho}'_{ab}(\vec{v},t,t_3+t_2-t_1)$ in a manner parallel to that for obtaining $\tilde{\rho}'_{ab}(\vec{v},t,t_1)$ in (46).

A solution of the same form as (48),

$$\tilde{\rho}'_{ab}(\vec{v},t,t_3+t_2-t_1) = -\tfrac{1}{2}i\exp[i\vec{x}'(t,t_3+t_2-t_1)\cdot\vec{v}] \times \exp[y'(t,t_3+t_2-t_1)], \tag{63}$$

again works and leads to Eq. (54) for $\dot{x}'(t,t_3+t_2-t_1)$ and $\dot{y}'(t,t_3+t_2-t_1)$ subject to initial conditions

$$\vec{x}'(t_3,t_3+t_2-t_1) = -\vec{x}(t_2,t_1), \tag{64a}$$

$$y'(t_3,t_3+t_2-t_1) = y(t_2,t_1), \tag{64b}$$

which may then be numerically integrated for any $t > t_3$. If $\Gamma(1-\alpha)t \ll 1$, then $x'(t,t_3+t_2-t_1) \ll k|(t-t_3-t_2+t_1)|$ for a sufficient range of t that the $\vec{x}'(t,t_3+t_2-t_1)$ terms may be dropped from the right-hand side of Eqs. (54) and the equations integrated to give

$$\vec{x}'(t,t_3+t_2-t_1) = -2\vec{x}(t_2,t_1) + 2\Gamma(1-\alpha)\vec{k}(k^2\Delta u^2)^{-1} \times \{1-\exp[-k^2(t-t_3-t_2+t_1)^2\Delta u^2/4]\}, \tag{65a}$$

$$y'(t,t_3+t_2-t_1) = 2y(t_2,t_1) - \Gamma(t-t_3-t_2+t_1) + \frac{2\Gamma}{k\Delta u}\int_0^{k(t-t_3-t_2+t_1)\Delta u/2} e^{-\eta^2}\,d\eta, \tag{65b}$$

where $x(t_2,t_1)$ and $y(t_2,t_1)$ are given by Eq. (57).

By combining Eqs. (65), (63), (45), (38), and (29), the quantities of interest $v(\vec{v},t)$ and $u(\vec{v},t)$ may be obtained as

$$v(\vec{v},t) = \tfrac{1}{2}NW_0(\vec{v})e^{-\Gamma_1 t}\exp[-i\delta(\omega_0)(t-2\tau)] \times \exp[i\vec{x}'(t,2\tau)\cdot\vec{v}]\exp[y'(t,2\tau)] + \text{c.c.}, \tag{66a}$$

$$u(\vec{v},t) = -(i/2)NW_0(\vec{v})e^{-\Gamma_1 t}\exp[-i\delta(\omega_0)(t-2\tau)] \times \exp[i\vec{x}'(t,2\tau)\cdot\vec{v}]\exp[y'(t,2\tau)] + \text{c.c.}, \tag{66b}$$

where τ is the mean interval time

$$\tau = \tfrac{1}{2}(t_3 + t_2 - t_1) \tag{67}$$

and x' and y' are given by Eqs. (65).

The polarization of the medium is easily calculated using Eqs. (11), (23), and (21) as

$$P(z,t) = ex_{ab}\int d^3v[u(\vec{v},t)\cos(kz-\omega_L t) + v(\vec{v},t)\sin(kz-\omega_L t)], \tag{68}$$

so that comparison with Eq. (3) gives

$$C(t) = ex_{ab}\int d^3v\, u(\vec{v},t), \tag{69a}$$

$$S(t) = ex_{ab}\int d^3v\, v(\vec{v},t). \tag{69b}$$

The echo field amplitude $E_C(z,t)$ appearing in Eqs. (4) and (12) is then obtained as a solution of Eq. (5a),

$$\left(\frac{\partial}{\partial z} + \frac{1}{c}\frac{\partial}{\partial t}\right)E_C(z,t) = -\frac{2\pi\omega_L}{c}S(t). \tag{5a}$$

Substituting (66a) into (69b) assuming a thermal distribution

$$W_0(\vec{v}) = (\pi u^2)^{-3/2}e^{-v^2/u^2}, \tag{70}$$

and recalling the definition (25) for $\delta(\omega_0)$, one finds

$$S(t) = ex_{ab}Ne^{-\Gamma_1 t}e^{y(t,2\tau)}\cos[(\omega_0-\omega_L)(t-2\tau)] \times \exp\{-[\vec{k}(t-2\tau)-\vec{x}'(t,2\tau)]^2u^2/4\}. \tag{71}$$

To solve Eq. (5a), we assume that the sample is thin enough so that the field builds up linearly along its length, i.e.,

$$E_C(z,t) = zA(t). \tag{72}$$

From Eq. (5a), one finds that $A(t)$ satisfies the equation

$$\frac{dA}{dt} + \frac{c}{z}A = -\frac{2\pi\omega_L}{z}S(t). \tag{73}$$

While this equation can be integrated to give $A(t)$, we can note that, at a given z, the field will vary in time on order $(\omega-\omega_L)^{-1}$ or $ku \approx 10^8$ sec^{-1} due to the time variation of $S(t)$ so that $|(dA/dt)/(c/z)A| \approx kuz/c \ll 1$ for our sample size of 10 cm. Thus, to sufficient approximation, $A(t) \approx -(2\pi\omega_L/c)S(t)$ and the field exiting the sample at $z = L$ is

$$E_C(L,t) \equiv E_C(t) = LA(t) = -(2\pi\omega_L/c)LS(t). \tag{74}$$

It can be seen from Eq. (71) that the echo signal has an envelope of width $\approx (ku)^{-1}$, that is modulated at frequency $\omega_0 - \omega_L$, and that the maximum echo amplitude occurs at $t = 2\tau$. Using Eqs. (74), (71), (67), (65), and (57), one may calculate the echo amplitude

$$E_C(t=2\tau) = -\frac{2\pi\omega_L}{c}ex_{ab}NL\exp\left\{-\Gamma_1 t - \Gamma t + \frac{4\Gamma}{k\Delta u}\int_0^{k\Delta ut/4}e^{-\eta^2}d\eta - 4\frac{\Gamma^2(1-\alpha)^2u^2}{k^2\Delta u^4}\left[1-\exp\left(-\frac{k^2\Delta u^2t^2}{16}\right)\right]^2\right\}, \tag{75}$$

where terms of order Γt_1 or $\Gamma(t_3 - t_2)$ have been neglected. The last term in the exponent will be negligible for the case of experimental interest

$$\Gamma/ku \ll 1, \tag{76}$$

so that the maximum absolute value of echo amplitude normalized to unity and denoted by $\bar{E}_C(t=2\tau)$ is

$$\bar{E}_C(t=2\tau) = \exp\left[-\Gamma_1 t - \Gamma t\left(1 - \frac{4}{k\Delta ut}\int_0^{k\Delta ut/4}e^{-\eta^2}d\eta\right)\right], \tag{77}$$

which is the result quoted in our earlier paper.

If one applies subsequent π pulses at time $t = (2n+1)\tau$ (n = positive integer) additional echoes will be produced at time $t = 2n\tau$ (Carr-Purcell-type experiment). It is a simple matter to convince oneself that the normalized maximum echo amplitude for this case, denoted by $\bar{E}_C(t=2n\tau, \text{CP})$ is given by Eq. (77) raised to the nth power, i.e.,

$$\bar{E}_C(t=2n\tau, \text{CP}) = \exp\left[-\Gamma_1 t - \Gamma t\left(1 - \frac{2}{k\Delta u\tau}\int_0^{k\Delta u\tau/2}e^{-\eta^2}d\eta\right)\right]. \tag{78}$$

The physical interpretation of Eqs. (77) and (78) will be given below after discussing the necessary modification of these results for the actual experimental situation.

E. Extension of the theory

In the actual experiment, it is possible to use field strengths such that the optimal conditions $\chi t_1 \approx \frac{1}{2}\pi$ and $\chi(t_3 - t_2) \approx \pi$ are maintained. Owing to power broadening, a monochromatic source excites a frequency bandwidth of order χ in a system of two-level molecules (see Appendix A for the details of the calculation). For the echo problem under consideration, the velocity bandwidth

that may be excited is of order

$$u_0 = \chi/k, \tag{79}$$

and will be centered around $v_z = -(\omega_s - \omega_L)/k$. In the simple model above, we assumed that u_0 was much greater than the thermal speed u so that the field interacted with the entire thermal distribution of molecules. Moreover, since $u_0 = \chi/k \gg u$, the power broadening was so great that the excitation spectrum was constant over the entire thermal distribution of velocities.

Experimentally, $u_0 \approx 10^3$ cm/sec while $u \approx 10^4$ cm/sec indicating that only a fraction of the molecules will interact with the laser field. The excitation spectrum for the molecules will *not* be constant but, instead, will have a width of order u_0. This, in turn, implies that if the field represents a π pulse for one velocity subgroup, it will not be a π pulse for another velocity subgroup. Thus, the simplification of assuming $\frac{1}{2}\pi$ and π pulses for the entire sample cannot be maintained.

Appendix A of this paper contains a calculation taking into account the finite excitation bandwidth. The results of that calculation with regard to the modification of Eq. (77) due to finite bandwidth and other than $\frac{1}{2}\pi$ and π pulses will be discussed below. In addition, we shall comment on modification of the Carr-Purcell signal (78) and on effects of degeneracy.

Finite bandwidth. The fact that only a fraction of the molecules are excited by the laser means that collisions, in addition to producing the changes in the Doppler phase factors discussed above, will also cause the excited velocity distribution of molecules to decay towards equilibrium. However, if $\Gamma t \Delta u^2/u_0^2 \ll 1$, as it is in our experiment, changes in the velocity distribution can be neglected[25] and Eq. (77) is not affected. If collisions did produce large Δu such that $\Delta u > u_0$, such collisions would remove molecules from the excitation bandwidth and would be reflected in an effective increase in the population loss rate Γ_1; however, this situation does not prevail according to the experiments of Sec. III.

Excitation spectrum. As is shown in Appendix A, the fact that there is an excitation spectrum rather than $\frac{1}{2}\pi$ and π pulses for the entire sample will lead to a modification of the shape of the echo signal, but not any change in its functional time dependence on pulse separation. In other words, the *relative* contribution of each velocity subgroup to the echo amplitude is unchanged as the pulse separation is varied. Thus, Eq. (77) can still be used to describe the dependence of echo amplitude on pulse separation.

Carr-Purcell signal. If all pulses after the first are anything but π pulses, the expression for the Carr-Purcell signal becomes quite complex since the overall amplitude factor of the echo signal varies with each subsequent echo. A formal analysis of the problem is not too difficult, but the algebra is tedious. The fact that the experimental data seems to follow Eq. (78) may imply that the pulses approximate π pulses fairly well.

Degeneracy effects. In reality, we are not dealing with a simple two-level system, but many two-level systems. If each of these two-level systems interacts independently with the field, they will contribute independent echo signals with somewhat different shapes but the same modulation frequency $(\omega_0 - \omega_L)$. In any event, the functional time dependence of maximum echo amplitude on pulse separation given by Eq. (77) will be unchanged. Possible interference effects such as two transitions sharing a common level or transfer of a dipole moment in a collision have not been included in the analysis, but it seems doubtful that these contribute significantly, particularly when the degeneracy is lifted by a Stark bias field.

F. Interpretation of the results

From the discussion above, we see that Eq. (77) may be used to analyze the two-pulse echo signal. The nature of the solution (77) depends on the value of the rms collisional change in the Doppler phase $k\Delta u\tau$. The asymptotic limits of (77) are

$$k\Delta u\tau \ll 1: \quad \bar{E}_C(t = 2\tau) \sim \exp[-\Gamma_1 t - \tfrac{1}{48}\Gamma t^3 (k\Delta u)^2], \tag{80a}$$

$$k\Delta u\tau \gg 1: \quad \bar{E}_C(t = 2\tau) \sim \exp\left(-\Gamma_1 t - \Gamma t + \frac{2\pi^{1/2}\Gamma}{k\Delta u}\right). \tag{80b}$$

The $\exp(-\Gamma_1 t)$ represents the decrease in echo amplitude due to population decay and is easily understood. The other terms in (80) represent the effects of velocity-changing collisions. Additional physical insight into these terms may be obtained by looking at a mathematically nonrigorous picture of echo formation.

The maximum echo signal arises when the net Doppler phase factor

$$\exp[i\vec{k}\cdot\vec{v}(t_2 - t_1) - i\vec{k}\cdot\vec{v}(t - t_3)] \tag{81}$$

goes to unity—i.e., the dephasing-rephasing process of echo formation has been accomplished. Collisions will produce a change in the Doppler phase factor which roughly goes as

$$H = \langle e^{i\vec{k}\cdot\Delta\vec{v}\tau} \rangle, \tag{82}$$

where $\langle \cdots \rangle$ represents a collision average. Let Δu be $\sqrt{2}$ times the rms change in velocity per collision. If $k\Delta u\tau \gg 1$ any collision produces de-

structive phase interference so that the only term which survives in Eq. (82) will be the one in which no collision occurs during the time $t=2\tau$. Since the associated probability is $e^{-\Gamma t}$, one finds

$$k\Delta u\tau \gg 1: \quad H \sim e^{-\Gamma t}, \tag{83a}$$

corresponding to (80b).

On the other hand, if $k\Delta u\tau \ll 1$, each collision produces only a small phase change such that

$$H \approx 1 - \tfrac{1}{2}k^2\langle(\Delta v)^2\rangle\tau^2,$$

where we have assumed $\langle\Delta\vec{v}\rangle=0$ for simplicity. The quantity $\langle(\Delta v^2)\rangle$ will be equal to (number of collisions in time $t=\Gamma t)\times[\langle\Delta v^2\rangle$ for one collision $=\frac{1}{2}\Delta u^2]$ so that

$$k\Delta u\tau \ll 1: \quad H \sim 1 - \tfrac{1}{4}k^2\Delta u^2\tau^2\Gamma t \approx \exp[-\Gamma t^3(k\Delta u)^2/16]. \tag{83b}$$

Except for numerical factors, Eqs. (83) agree with the asymptotic forms (80) of the transport equation solution. Thus, the decrease in echo amplitude due to velocity-changing collisions results simply because the collisions destroy the perfect Doppler phase cancellation which would have occurred had the collisions been absent.

We note by expanding the exponential in (50) and carrying through the calculation as above, it is easy to derive the following formula for the echo amplitude valid for any type Brownian motion collision kernel $W(\vec{v}'\to\vec{v})$ when $k\Delta u\tau \ll 1$

$k\Delta u\tau \ll 1$:

$$\bar{E}_c(t=2\tau) = \exp\left(-\Gamma_1 t + 2\sum_{m=1}^{\infty}\frac{(-1)^m(\tau)^{2m+1}}{(2m)!} \times \int d^3v W(\vec{v}\to\vec{v}')[\vec{k}\cdot(\vec{v}-\vec{v}')]^{2m}\right). \tag{84}$$

In addition, Eq. (83a) will still be valid for $k\Delta u\tau \gg 1$ so that Eqs. (84) and (83a) generalize our results to any Brownian motion kernel. This argument substantiates our claim that the t^3 and t dependence associated with velocity-changing collision is independent of the choice of collision kernel.

Previous theories of echo formation employed a Fokker-Planck equation (FPE) rather than a transport equation to treat collisions.[11,16,21,24] For times $\Gamma t(1-\alpha)\ll 1$, such theories give the limiting form (80a) for the echo amplitude rather than the entire Eq. (77). It has been shown that the transition from the transport equation to the FPE is valid only if a single collision produces a negligible change in the distribution-function or density-matrix elements. For the echo problem, the effect of a single collision is negligible only if $k\Delta u\tau \ll 1$. Thus one can expect the FPE treatment to fail (as it does) when $k\Delta u\tau \gtrsim 1$.

Finally, we might mention the Carr-Purcell signal (78). If one can use short pulse separations τ such that $k\Delta u\tau \ll 1$, Eq. (78) will reduce to

$$k\Delta u\tau \ll 1: \quad \bar{E}_c(t=2n\tau, \mathrm{CP}) \sim e^{-\Gamma_1 t}, \tag{85}$$

and the Carr-Purcell signal can be used to determine the population decay rate Γ_1.

III. T_1 MEASUREMENTS

Photon-echo experiments, as we shall see in Sec. IV, allow a direct and quantitative study of molecular-velocity-changing collisions and a test of the validity of (77). In this section, we consider the phenomenological damping T_1 which also enters (77) through the diagonal density-matrix equations of motion (13) where it is defined. The principal contribution to T_1 is due to the molecular transit time across the laser beam and to jumps in molecular quantum state arising from inelastic collisions. Clearly, if the velocity-changing collision part of (77) is to be examined quantitatively, an independent measurement of T_1 is required. We may also compare T_1 with the relaxation time observed in optical multiple pulse (Carr-Purcell) echoes[8] and coherent Raman-beat experiments[5,6] where the importance of phase-interrupting collisions and other conclusions can be reached.

A. Apparatus

The experimental arrangement employed throughout this article is shown in Fig. 3. It utilizes the Stark switching method[4] that has now allowed the observation of optical nutation,[4] photon echoes involving two[4] or multiple pulses (stimulated[26] and Carr-Purcell echoes[8]), optical free induction decay (FID),[7] coherent Raman beats,[5,6] optical adiabatic fast passage,[9,27] the optical analog of spin locking,[28] and FID interference pulses.[10]

A molecular gas sample that is Stark tunable is irradiated by a continuous wave CO_2 laser beam. Electronic pulses are applied repetitively to the sample thereby switching the molecular level structure in or out of resonance with a fixed laser frequency, and a particular coherent transient effect can be selected simply by varying the pulse sequence.

Transient light signals that are emitted by molecules switched out of resonance propagate in the forward direction and are monitored together with the transmitted laser beam by a germanium-gold-doped photodetector (rise time: 30 nsec). Heterodyne detection is possible in the Raman-beat and photon-echo experiments to be described since the emission signal is Stark shifted from the laser

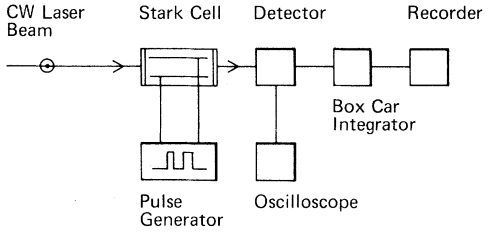

FIG. 3. Method for observing coherent optical transients following a sequence of Stark pulses (from Brewer and Shoemaker, Ref. 4).

frequency; this increases the echo signal 1000-fold and also enhances detection sensitivity. Optical nutation ringing patterns are detected also by monitoring the transmitted beam when a Stark pulse suddenly switches molecules into resonance. The detector output is amplified 1000 times with a preamplifier having a 5 nsec risetime, and is stored and signal averaged in a Princeton Applied Research 160 box car integrator before being displayed on an x-y recorder.

Single or multiple electronic pulses with a 5 nsec risetime and a variable width (0.1–300 μsec), amplitude (0–200 V) and repetition frequency (2.5–80 kHz) are applied to an optical Stark cell. Single or double pulses are derived from a pulse generator that uses TTL logic elements, and a gated n pulse train from a Tektronix 2101 pulse generator. The time scale is calibrated by a Tektronix 2901 time mark generator, accurate to 3 parts per million.

A free running, frequency stable CO_2 laser, which has been described previously,[29] is made to oscillate in the lowest-order mode on the $P(32)$ laser line at 1035.474 cm^{-1}; the line is selected by adjustment of a rotatable grating at one end of the optical cavity. Fine-frequency tuning over the 50-MHz CO_2 Doppler width is accomplished piezoelectrically. The laser beam, ~1 W of continuous power, is expanded to ~1 cm diameter by a Galilean telescope to lengthen the molecular time of flight across it. The radiation is linearly polarized, perpendicular to the Stark field, so that $\Delta M = \pm 1$ optical selection rules apply.

The same vibration-rotation transition of $^{13}CH_3F$ reported in our preliminary findings[8] is examined here as well. This is the fundamental ν_3 band $R(4)$ line, $(J,K) = (4,3) \rightarrow (5,3)$ that overlaps the $P(32)$ CO_2 laser line at 9.66 μm. Gas samples that were 90% enriched in $^{13}CH_3F$ were used, and pressures were measured in the mTorr range with an MKS Baratron gauge. The Stark cell had an active optical path length of 10 cm and for most of the measurements a 0.602 56-cm gap spacing.

B. Delayed optical nutation

Figure 4 illustrates a new optical technique for obtaining T_1 that is based on the nutation effect. A molecular gas sample that is Stark tunable is irradiated under steady-state conditions by a continuous laser beam, thereby burning a hole within the Gaussian velocity distribution. When a Stark pulse of width τ appears, a partially saturated velocity group $\vec{v}$ is suddenly switched out of optical resonance with the laser frequency and emits a short-lived FID signal. Simultaneously, a second velocity group $\vec{v}'$, which need not concern us, is switched into resonance giving the first optical-nutation pattern of Fig. 4. When the pulse terminates, the initial velocity group $\vec{v}$ is switched back into resonance and generates the second nutation pattern. The amplitude of this delayed nutation which is of interest depends on the population of the group $\vec{v}$ at the end of the pulse and thus on the extent to which the hole has been filled during the pulse interval. (Note that the group $\vec{v}'$ simultaneously emits a FID signal which is unimportant because it is short lived.) The dependence of the nutation amplitude on pulse width τ, derived in Appendix B, is proportional to the population difference

$$w(\tau) = w_0 - [w_0 - w(0)]\, e^{-\tau/T_1}, \tag{86}$$

where $w(\tau) \equiv [\rho_{aa}(\tau) - \rho_{bb}(\tau)]$ at the end of the pulse, $w(0)$ is the population difference at time zero preceding the pulse during steady-state excitation, and w_0 is the population difference in the absence of radiation. We see that the second nutation pattern of Fig. 4 will grow with increasing pulse width, according to (86), and that T_1 may be

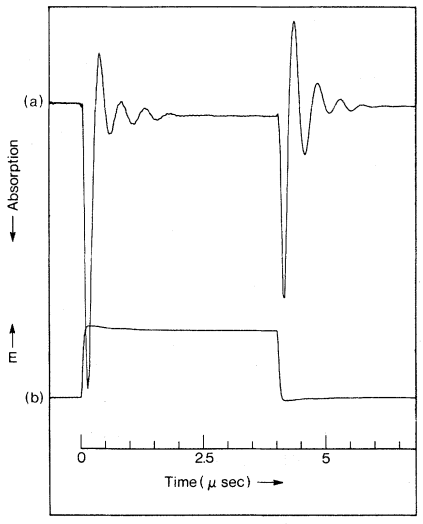

FIG. 4. Optical nutation in $^{13}CH_3F$. Pulse amplitude $E = 35$ V/cm (from Brewer and Shoemaker, Ref. 4).

readily obtained from the envelope function.

The above discussion presumes that the saturation hole is filled dominantly by molecules that have suffered a change in quantum state rather than by a molecular velocity-diffusion mechanism. The latter process as the present study shows is indeed a much slower effect. In particular, the Raman-beat measurements of Sec. IIIC remove any doubt concerning this point. We also note that this T_1 measurement is simpler theoretically and experimentally than the two-pulse nutation technique described in our previous letter.[8]

The T_1 nutation measurements carried out as a function of $^{13}CH_3F$ pressure are summarized in the linear relation

$$1/T_1 = 0.080 + 0.089P\ \mu\text{sec}^{-1} \tag{87}$$

for P in mTorr. As expected, T_1 is found to be independent of laser intensity. The intercept of 0.080 μsec^{-1} corresponds to the molecular time of flight across the 0.6 cm transverse dimension of the Stark cell. The collision term compares to $0.076P\ \mu\text{sec}^{-1}$ of Schmidt *et al.*[8] and to the microwave result $0.095P\ \mu\text{sec}^{-1}$ of Jetter *et al.*[30] The average of the three values gives $(0.087 \pm 0.007)P\ \mu\text{sec}^{-1}$.

The pressure dependence of (87) signifies collision-induced jumps in the rotational (J) and space quantized (M) states arising from the long-range permanent dipole-dipole force of $^{13}CH_3F$ pairs. Using (87), we calculate a total inelastic cross section $\sigma = 1/T_1 Nu\sqrt{2}$ of 500 Å^2. The results of Brewer, Stenholm, and Shoemaker,[31] using collision-induced optical double resonance, show that 15% of the collisions contributing to T_1 (for this same optical transition) produce a change in M state while (J, K) remains fixed. Their work also confirms a conclusion of this article, namely, that the molecular velocity suffers only slight changes for collisions that tip only the angular-momentum vector. The remaining 85% of the collisions influencing T_1 presumably involves quantum changes both in J and M and a greater smearing of molecular velocity.

C. Coherent Raman beats

The coherent Raman-beat effect[5,6] is particularly interesting in these studies because its decay time is independent of velocity-changing collisions. This contrasts sharply with the faster dephasing behavior of the two-pulse echo to be discussed and supports the idea that photon echo experiments are profoundly influenced by molecular collisions that alter velocity. The Raman decay may also be compared with the T_1 measurement of Sec. III B in determining to what extent phase interrupting collisions are important.

Raman beats are monitored in these studies using the experimental configuration of Fig. 3 as described in Ref. 5. For the purpose of discussion, let us consider only three levels where two of them, labelled 1 and 2, are initially degenerate in M and are in superposition with level 3 because of excitation with laser light. This constitutes the steady-state preparative stage preceding the Stark pulse. Sudden application of a step function Stark field removes the 1-2 level degeneracy and coherent forward Raman scattering follows, the laser now being nonresonant with either the 1-3 or 2-3 transition. Both Raman and laser light coincide spatially producing a coherent beat signal at the detector and with a frequency equal to the Stark splitting $\omega_{12} = (E_1 - E_2)/\hbar$. Brewer and Hahn[6] have shown that this transient signal decays as $\exp(-t/T_2)$, independent of molecular velocity, where τ_2 is the phenomenological Raman dephasing time introduced in the equation of motion for the off-diagonal element ρ_{12}. It is not evident a priori that

$$\tau_2 = T_1 \tag{88}$$

because collisions might shift the level spacing ω_{12}, disrupting the phase of ρ_{12} and shortening τ_2. However, simultaneous measurements of τ_2 and T_1 as a function of pressure show indeed that they are the same to within an uncertainty of ~3%. Here, the τ_2 values have been corrected slightly for the rate at which the Raman transition is driven by the laser; the observed dependence of decay rate[6] on laser intensity I is of the form suggested by Brewer and Hahn

$$1/\tau_2(\text{eff}) = 1/\tau_2[1 + 0.076I\,(\text{W/cm}^2)].$$

In view of the experimental support of (88), we conclude that phase-interrupting collisions have a negligible effect on ρ_{12} and therefore on Raman beats. Clearly, the Raman-beat effect provides an alternate way of determining T_1.

The result that $\tau_2 = T_1$ also confirms that a T_1 measurement is insensitive to velocity-changing collisions. Another implication of this specific result, discussed further in Sec. IV, is that large jumps in velocity are unimportant for elastic CH_3F-CH_3F collisions.

D. Optical Carr-Purcell echoes

The optical analog[8] of Carr-Purcell multiple-pulse spin echoes[13] is demonstrated in Fig. 5 for the Stark-pulse sequence shown. Under appropriate circumstances, this method also provides a value for T_1 when the dephasing time T_2 associated with the off-diagonal element ρ_{ab} satisfies

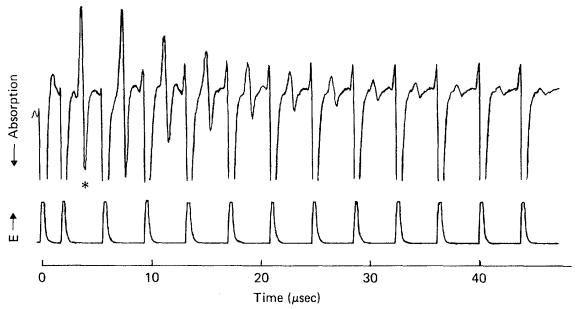

FIG. 5. Optical Carr-Purcell echoes in $^{13}CH_3F$. The first echo of the sequence is marked by an asterisk. Conditions are the same as in Fig. 6 (from Schmidt, Berman, and Brewer, Ref. 8).

$$T_2 = T_1. \tag{89}$$

Carr-Purcell echoes were developed in NMR to minimize the dephasing of ρ_{ab} arising from spectral diffusion. In solids, spectral diffusion results from local fluctuating dipolar fields on a spin site due to its neighbors.[16] In liquids, Brownian motion causes the nuclear spins to diffuse through the gradient of an external magnetic field.[11] For either case, the transition frequency in this two-level problem undergoes small chaotic variations, describable by a diffusion law, that disrupts the coherent behavior of ρ_{ab}. In the optical case treated here, the transition frequency of gaseous molecules wanders randomly by small increments because of elastic collisions that alter the molecular velocity and hence the Doppler shift of the emitted light. We now show that the dephasing caused by velocity-changing collisions can be virtually eliminated in a Carr-Purcell experiment.

Spectral diffusion of gas molecules in a two-pulse echo experiment leads to the nonlinear decay law of (80a)

$$e^{-Kt^3} = e^{-8K\tau^3},$$
$$K = \Gamma k^2 \Delta u^2/48, \tag{90}$$

where $t = 2\tau$. For the Carr-Purcell n-pulse echo train, the amplitude of the last echo at time $t = 2n\tau$ is proportional to the nth power of (90)

$$(e^{-8K\tau^3})^n = e^{-Kt^3/n^2}. \tag{91}$$

We see that over the same time interval t, the exponent of (91) is smaller than that of (90) by the factor $1/n^2$ and the Carr-Purcell method can give a much longer decay time. It is also clear that while the velocity diffusion contribution (91) is never zero, it can be made vanishingly small by reducing τ.

On the other hand, the linear decay term e^{-t/T_2} is the same in either a two-pulse or multiple-pulse echo sequence, and therefore, it gives a residual damping in a Carr-Purcell measurement. Molecular collisions that shift the transition frequency will introduce phase interruptions in ρ_{ab}, causing T_2 to be less than T_1, in general. However, in the present experiments (Fig. 5), the envelope function of the Carr-Purcell echoes when plotted in Fig. 6 falls on top of the T_1 nutation results of III B. This shows that $T_2 = T_1$, and as in the case of Raman beats, collisional phase interruptions are negligible.

Furthermore, we see that all three methods described in Secs. III B–III D are independent of velocity-changing collisions and agree well with the value of T_1 given in (87), to within a 3% uncertainty.

IV. TWO-PULSE ECHOES

A typical two-pulse echo[4] is shown in Fig. 7 and its decay behavior as a function of delay time $t = 2\tau$ is plotted in the lower curve of Fig. 6. The first and second Stark-pulse widths are 100 and 200 nsec, and a Stark bias field of 83 V/cm has been applied to suppress the coherent Raman-beat effect. The decay is not a simple exponential but shows an unusual time dependence that departs first slowly from the T_1 behavior (upper curve) and then more rapidly at longer times. Closer examination shows that there are two limiting time regimes of the form

$$e^{-Kt^3}, \text{ for short times;} \tag{92a}$$
$$e^{-\Gamma t}, \text{ for long times.} \tag{92b}$$

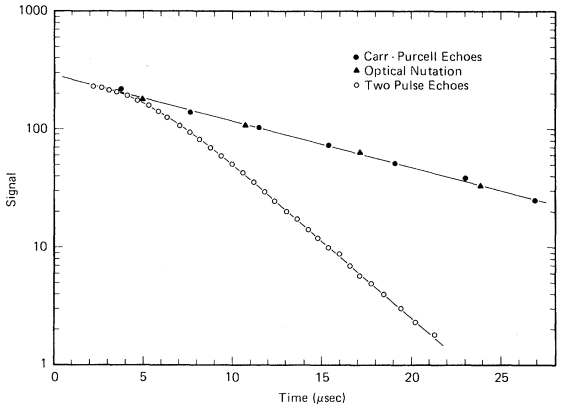

FIG. 6. Decay curves of optical coherent transients in $^{13}CH_3F$. The pressure is 0.32 mTorr, the laser beam diameter matches a 1.3-cm Stark spacing, the Stark pulses are 40 V/cm and a bias field of 80 V/cm is added to remove any complication of level degeneracy. The expanded laser beam's power density is about 350 mW/cm^2. The time axis is the total elapsed time t for each experiment, so that $t = 2\tau$ in a two-pulse echo or $t = 2n\tau$ in an n-pulse echo train (from Schmidt, Berman, and Brewer, Ref. 8).

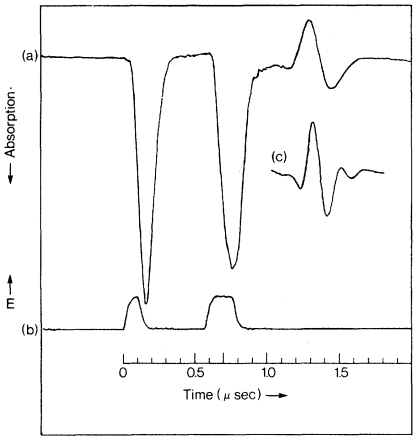

FIG. 7. Two-pulse photon echo in $^{13}CH_3F$. (a) Optical response, (b) Stark pulse sequence with $E = 35$ V/cm (from Brewer and Shoemaker, Ref. 4).

The long-term linear decay is clearly evident in Fig. 6 over two decades of signal amplitude, but the cubic time dependence is better shown in Fig. 8 when replotted on a t^3 time axis.

The observed functionality in time (92) is precisely what is predicted by Eqs. (80a) and (80b). The agreement constitutes primary evidence that elastic molecular collisions involving small changes in velocity play a crucial role in photon-echo measurements. The departure of the echo from the T_1 decay in Fig. 6 is due solely to the velocity-changing mechanism and is consistent with the experiments of Sec. III where T_1 is shown to be independent of elastic collisions.

It is interesting at this point to compare the effect of spectral diffusion on spin echoes in molecular liquids. In that case, the same e^{-Kt^3} law is obeyed, but the long-time exponential $e^{-\Gamma t}$

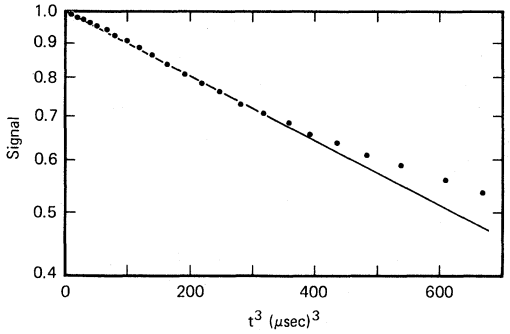

FIG. 8. Decay curve of two-pulse photon echoes in the region of short times where the t^3 behavior is evident out to 400 μsec^3; replotted from the lowest curve of Fig. 6 with the T_1 decay subtracted (from Schmidt, Berman, and Brewer, Ref. 8).

decay witnessed here never appears. To understand this behavior notice that, for a dilute gas, echoes are formed in the t^3 region by all active molecules whether they have collided or not, whereas in the t region only the collision free molecules form echoes. The ones that collide contribute to echo formation only for short times when the phase excursions are small, $kt\,\Delta u < 1$. This accounts for the short time regime of (80a). As the pulse delay advances so that $kt\,\Delta u \geq 1$, colliding molecules have completely dephased and no longer participate in the echo. The group that didn't undergo collisions obviously generates an echo, but its survival probability diminishes with time as $e^{-\Gamma t}$, in accordance with the observed long-time behavior of (80b). On the other hand for a liquid, collisions are so frequent and the phase jumps so small that the phase excursion remains small compared to unity; therefore, only the t^3 region is seen.

According to (80) and the above argument, the transition from the short to the long-time regime should occur when the Doppler phase factor

$$k\bar{t}\,\Delta u \sim \pi, \tag{93}$$

the result being independent of gas pressure. Pressure-dependent studies seem to confirm this prediction where the intermediate time $\bar{t} \sim 6$ μsec, as can be seen in Fig. 6. This implies that the characteristic jump in velocity of a CH_3F-CH_3F collision is

$$\Delta u = 80 \text{ cm/sec}. \tag{94}$$

We shall show later that this value agrees well with a more careful analysis of the echo-decay data.

Another feature expressed in the velocity-dependent collision term of (77) is the linear pressure dependence contained in the Γ factor. We find that the collision parameter Γ, as derived from the observed long-time decay $e^{-\Gamma t}$, fully confirms the expected linear pressure dependence where examples are given in Fig. 9. Similar measurements in the short-time region reveal the same linear pressure behavior in $K = \Gamma k^2 \Delta u^2/48$ for the e^{-Kt^3} decay.

Before proceeding further, one may question the importance of collisions where the velocity-change falls outside the detection bandwidth of a two-pulse echo experiment. It is apparent that these collisions would contribute to T_1 but not to the Raman-beat decay τ_2 since τ_2 is independent of velocity-changing collisions in general. The fact that $\tau_2 = T_1$, following (88), allows us to conclude that these collisions are not important and have no influence on the present echo studies.

A. Intensity-dependent dephasing

One puzzling aspect of the echo measurement that still remains is an intensity-dependent dephasing effect not predicted by (77). The phenomenon is best characterized by Fig. 9 which shows a family of Γ-vs-pressure curves as a function of laser power. We see that increasing the laser intensity, in the range 0–1 W/cm^2, shifts the intercept of Γ upward but does not influence its pressure-dependent slope noticeably. The decay parameter K shows a similar shift in its intercept with intensity. At a given pressure P, we find that Γ and K depend on laser intensity I in the following way

$$\Gamma(P,I)=\Gamma(P)+\theta I,$$
$$K(P,I)=K(P)+\Phi I, \tag{95a}$$

where $\Gamma(P)$ and $K(P)$ are intensity independent and

$$\theta=0.23\ \mu\text{sec}^{-1}\text{W}^{-1}\text{cm}^2,$$
$$\Phi=1.1\times10^{-3}\ \mu\text{sec}^{-3}\text{W}^{-1}\text{cm}^2. \tag{95b}$$

One obvious intensity-dependent mechanism is an off-resonance driving effect. Because laser radiation is always present throughout the measurement, molecules that produce an echo when switched out of resonance can be driven slightly in their off-resonant condition. However, estimates of this effect do not appear to influence the echo decay rate in an intensity-dependent manner.

Another possibility is that the Raman-beat effect could occur simultaneously and compete with echo formation. However, the Raman-beat effect can be suppressed with an adequate Stark bias field, as in the present two-pulse echo experiments, so that the required pulse preparation cannot take place. Even more convincing are experiments with $\Delta M=0$ optical selection rules where the Raman effect is excluded and yet the intensity dephasing still persists.

Other possible explanations of this anomaly have not been pursued as yet.

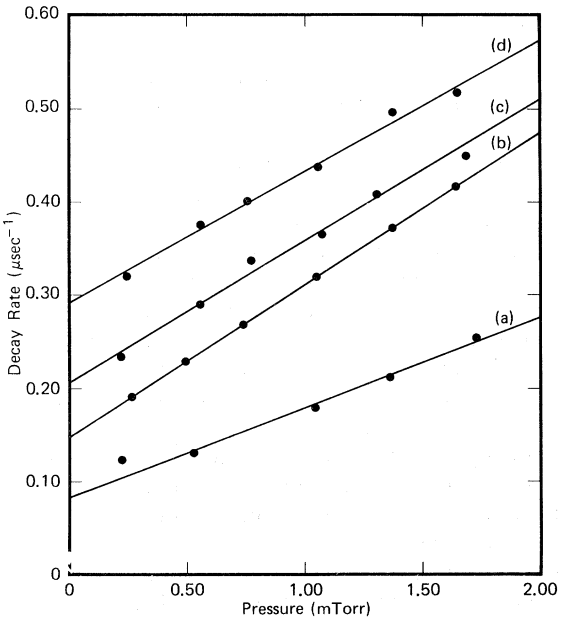

FIG. 9. $^{13}CH_3F$ decay rates $1/T_1$ vs pressure (curve a) and $(1/T_1+\Gamma)$ versus pressure and laser intensity: curve b, (307 mW/cm^2); curve c, (660 mW/cm^2); and curve d (1110 mW/cm^2).

B. Collision parameters

In the absence of understanding the above intensity dephasing effect, we make use of the empirical quantity (95), thereby obtaining collision parameters in the zero-laser-power limit

$$\Gamma(P)=0.074P\ \mu\text{sec}^{-1},$$
$$K(P)=4.9\times10^{-4}P\ \mu\text{sec}^{-3}, \tag{96}$$

with P in mTorr. Here, Γ and K are derived from the observed long- and short-time two-pulse echo decay behavior, Figs. 6 and 7 for example, after subtracting the measured $1/T_1$ contribution. Measurements as a function of laser intensity allow extrapolation to zero intensity and give (96).

We are now in a position to determine the $^{13}CH_3F$-$^{13}CH_3F$ collision parameters

$$\sigma=430\ \text{Å}^2, \tag{97a}$$
$$\Delta u=85\ \text{cm/sec}, \tag{97b}$$

for velocity-changing collisions where the total elastic collision cross section is defined by $\sigma=\Gamma/Nu\sqrt{2}$ and $\Delta u=(1/k)(48K/\Gamma)^{1/2}$ from the definition (90). Here, $k=6.50\times10^3$ cm^{-1}, $u=3.75\times10^4$ cm/sec, and Γ and K are taken from (96). Measurements of Γ and K at different pressures reveal that Δu is pressure independent in agreement with our collision model. We note that the magnitude of Δu agrees with our previous estimate (93), but it is about a factor of 2 smaller than the preliminary measurement of Schmidt *et al.*[8] which is considered less reliable.

A self-consistency check of the slope method used to obtain (97) can be obtained by noting that the echo amplitude in the long-time regime (80b) displays the extrapolated zero-time intercept

$$\bar{E}_c(t=0)=\exp(2\pi^{1/2}\Gamma/k\Delta u). \tag{98}$$

A value of Δu may then be derived from (98) for each decay curve using the observed intercept and Γ. We find in this way that the average value is $\Delta u=50$ cm/sec, in reasonable agreement with

(97b).

In considering the errors involved in these measurements, we should note that the measured quantity of interest is the difference between T_1 and the two-pulse echo decay. Since this difference is a small quantity in the short-time regime, it is more susceptible to error than in the long-time behavior. This implies a larger fractional uncertainty in Δu than in Γ. The remaining uncertainty lies in the intensity extrapolation which is difficult to assess at present.

V. SUMMARY

We have shown that the optical line profile of a molecular gas may be decomposed into elastic and inelastic collision contributions through coherent optical transient experiments. The velocity diffusion or elastic part is detected by two-pulse echoes and is emphasized here in view of the absence of previous experiments and relevant theoretical predictions.

The echo decay function, which provides a signature for the velocity-changing collision mechanism, is characterized by two limiting time regimes, e^{-Kt^3} for short times and $e^{-\Gamma t}$ for long times. The cubic decay law is due to molecules that collide elastically, and applies when the Doppler-phase excursions are small, $k\Delta u\tau \ll 1$. The resulting diffusion in velocity space can be described by a solution of the Fokker-Planck equation as in spin-echo experiments where molecular liquids are subject to Brownian motion. In the long-time regime, $k\Delta u\tau \gg 1$, most of the molecules that collide have by now dephased and don't contribute to echo formation. The echo is then due to those molecules that didn't collide, their survival probability being an exponential in time. Here as in the intermediate time region, the Fokker-Planck solution fails.

The entire time dependence, which is unknown heretofore, follows however, from a solution of the Boltzmann transport equation. Our experiments suggest a Brownian-motion weak-collision model, and for convenience we have adopted the Keilson-Storer kernel

$$W(\vec{v}' \to \vec{v}) = \Gamma(\pi\Delta u^2)^{-3/2} e^{-(\vec{v}-\alpha\vec{v}')^2/\Delta u^2},$$

which allows an analytic solution. In terms of these collision parameters, the echo measurements of $^{13}CH_3F$ reveal that root two times the rms change in velocity per collision is only $\Delta u = 85$ cm/sec and that the total elastic collision cross section is $\sigma = \Gamma/Nu\sqrt{2} = 430$ Å^2. From the above Δu value and (33) we see that $(1-\alpha) = 2.6\times10^{-6}$ so that the velocity jumps are closely clustered about the initial velocity as required in a weak-collision model. Furthermore, it follows that an arbitrary initial velocity approaches a thermal-equilibrium distribution[32] as $\exp(-\beta t)$ in a time $\beta^{-1} = [\Gamma(1-\alpha)]^{-1} = 5$ sec which contrasts greatly with the time scale of an echo experiment $\Gamma^{-1} \sim 14$ μsec at 1 mTorr pressure.

It might be argued that the echo measurement is insensitive to large jumps in velocity that fall outside the detection bandwidth and therefore would go unnoticed. However, *coherent Raman beat* and T_1 decay measurements deny this possibility. Such large velocity changes would limit the molecule-optical interaction time and would contribute to a T_1 decay which is determined here in a *delayed nutation measurement*. The Raman decay time τ_2, on the other hand, is independent of collisions that induce changes in velocity. Since the experiments show that $\tau_2 = T_1$, it must be concluded that T_1 is independent of *all* velocity-changing collisions, and large velocity jumps are of no consequence in an echo or any other measurement. This further implies that when a hole is burned within the Doppler profile, velocity equilibrium is established not primarily by elastic collisions but rather by the inelastic ones. The total cross section for inelastic collisions,[33] as determined from T_1 measurements, is found to be 500 Å^2.

Another competing mechanism to be considered is that of "phase-interrupting collisions." Had this mechanism prevailed, collisions would be state dependent, and the echo signal would have been of the form e^{-t/T_2} with no e^{-Kt^3} dependence, in contradiction to the observations. Phase interruptions are also ruled out by *optical Carr-Purcell echo measurements* which give a direct measure of T_2 and would reflect such phase changes while being independent of elastic collisions. Since we find that $T_2 = T_1$ where T_1 cannot depend on phase interruptions, we can exclude this possibility as well. The result is physically reasonable for a vibration-rotation transition because upper and lower transition states are not expected to show a significant relative or absolute frequency shift. On the other hand, for an electronic transition it would be of interest to see if the two-echo pulse shows a simple exponential decay arising from phase interruptions and hence no contribution from velocity changes.

The pressure-dependent part of T_1 represents still other collision processes, namely, those that involve population changes and thus a change in quantum state, the most conspicuous being jumps in molecular rotation (J) and orientation (M). Recent optical double-resonance studies[31] of $^{13}CH_3F$ have indicated efficient transfer among neighboring M states, due to the permanent dipole-

dipole interaction. This interaction presumably plays the dominant role in elastic collisions as well. A more complete theoretical treatment would require the replacement of the collision kernel by a detailed interaction description, and in fact, optical coherent transients could be used to investigate the nature of the collision interaction.

Thus, the present experimental and theoretical study covers several new aspects of molecular collisions. It represents the first detailed examination of velocity-changing collisions by coherence methods and without the complication of Doppler broadening.

ACKNOWLEDGMENT

We greatly appreciate the expert technical assistance of K. L. Foster in all phases of our experiments.

APPENDIX A: GENERALIZATION OF ECHO CALCULATION

In this Appendix, we generalize the echo calculation of Sec. II to allow for arbitrary pulse widths and a realistic velocity bandwidth of the sample molecules. The calculation parallels that of the text for the simple model and we consider the various time regions of Fig. 2. We again assume that the time intervals t_1 and $(t_3 - t_2)$ are small enough to neglect any collisional relaxation during these intervals.

a. $0 < t < t_1$. It follows directly that the set of coupled equations represented by Eq. (30) with $\omega = \omega_s$ and with the collision terms dropped can be solved to yield

$$\vec{B}'(\vec{v}, t_1) = [u'(\vec{v}, t_1), v'(\vec{v}, t_1), w'(\vec{v}, t_1)],$$

$$u'(\vec{v}, t_1) = 2N W_0(\vec{v}) \frac{\chi \delta(\omega_s)}{[\xi(\omega_s)]^2} \sin^2(\theta_{10}/2), \tag{A1a}$$

$$v'(\vec{v}, t_1) = -NW_0(\vec{v}) \frac{\chi}{\xi(\omega_s)} \sin\theta_{10}, \tag{A1b}$$

$$w'(\vec{v}, t_1) = -NW_0(\vec{v}) \left[\left(\frac{\delta(\omega_s)}{\xi(\omega_s)} \right)^2 + \left(\frac{\chi}{\xi(\omega_s)} \right)^2 \cos\theta_{10} \right], \tag{A1c}$$

where

$$\theta_{ij} = \xi(\omega_s)(t_i - t_j) \tag{A2}$$

and

$$\xi(\omega) = \{ [\delta(\omega)]^2 + \chi^2 \}^{1/2}. \tag{A3}$$

One notes that the bandwidth of molecules excited by this pulse is on the order of $\delta(\omega) \approx \chi$.

b. $t_1 < t < t_2$. In this region, $\omega = \omega_0$ which is assumed to be so far off-resonance for the molecules excited by the first pulse that we can effectively take $\chi = 0$. Proceeding as in the text, we find that we must solve Eq. (30) for $\vec{B}'(\vec{v}, t)$ with $\Omega = \Omega_0$ given by Eq. (37) subject to the initial condition (A1) for $\vec{B}'(\vec{v}, t_1)$. The new initial condition differs from that of the simple model of the text in that its velocity dependence is no longer that of the thermal-equilibrium distribution $W_0(\vec{v})$, but rather $W_0(\vec{v})$ multiplied by a velocity distribution with width of order

$$u_0 = \chi/k. \tag{A4}$$

As we trace the evolution of $\vec{B}'(\vec{v}, t)$ in this time regime, two nonseparable physical processes will be occurring. First, there will be the collision-induced changes in the Doppler phase factor discussed in the text. In addition, there will be the relaxation of the initial velocity distribution given by Eq. (A1) to the equilibrium distribution $W_0(\vec{v})$. One can consistently treat both processes,[32] but the mathematics becomes quite involved.

There is a simplification possible for the case of physical interest. In a previous paper,[25] it has been shown that, provided $\Delta u/u_0 \ll 1$, the velocity *distribution* will be unchanged for times t such that

$$\Gamma t (\Delta u^2/u_0^2) \ll 1. \tag{A5}$$

In our experiment, $\chi t_1 \approx 1$, $t_1 \approx 10^{-7}$ sec, $k \approx 2\pi \times 10^3$ cm^{-1} giving $u_0 \approx 10^3$ cm/sec which, combined with the value $\Delta u \approx 100$ cm/sec, leads to $(\Delta u/u_0)^2 \approx 0.01$. Thus, for the range of interest of our experiment ($\Gamma t \approx 1$), Eq. (A5) is satisfied and we shall make negligible error by assuming the velocity distribution is unchanged throughout the experiment. In that case, the entire calculation of the text may be repeated to yield

$$u'(\vec{v}, t_2) = \tfrac{1}{2}[u'(\vec{v}, t_1) - iv'(\vec{v}, t_1)] \exp[-i\delta(\omega_0)(t_2 - t_1)] \times \exp[i\vec{x}(t_2, t_1) \cdot \vec{v}] \exp[y(t_2, t_1)] + \text{c.c.}, \tag{A6a}$$

$$v'(\vec{v}, t_2) = \tfrac{1}{2}[u'(\vec{v}, t_1) - iv'(\vec{v}, t_1)] \exp[-i\delta(\omega_0)(t_2 - t_1)] \times \exp[i\vec{x}(t_2, t_1) \cdot \vec{v}] \exp[y(t_2, t_1)] + \text{c.c.}, \tag{A6b}$$

$$w'(\vec{v}, t_2) = w'(\vec{v}, t_1), \tag{A6c}$$

with $u'(\vec{v}, t_1)$, $v'(\vec{v}, t_1)$, and $w'(\vec{v}, t_1)$ given by Eq. (A1) and $\vec{x}(t_2, t_1)$ and $y(t_2, t_1)$ given by Eq. (57).

c. $t_2 < t < t_3$. We solve Eqs. (30) with $\omega = \omega_s$ and neglecting the collision terms, subject to initial

conditions at $t=t_2$ given by Eqs. (A6), to obtain

$$u'(\vec{v},t_3)=\left[\left(\frac{\delta(\omega_s)}{\xi(\omega_s)}\right)^2\cos\theta_{32}+\left(\frac{\chi}{\xi(\omega_s)}\right)^2\right]u'(\vec{v},t_2)$$
$$-\frac{\delta(\omega_s)}{\xi(\omega_s)}\sin\theta_{32}v'(\vec{v},t_2)$$
$$-2\frac{\chi\delta(\omega_s)}{\xi(\omega_s)^2}\sin^2(\tfrac{1}{2}\theta_{32})w'(\vec{v},t_2), \qquad \text{(A7a)}$$

$$v'(\vec{v},t_3)=\cos\theta_{32}v'(\vec{v},t_2)+\frac{\delta(\omega_s)}{\xi(\omega_s)}\sin\theta_{32}u'(\vec{v},t_2)$$
$$+\frac{\chi}{\xi(\omega_s)}\sin\theta_{32}w'(\vec{v},t_2), \qquad \text{(A7b)}$$

$$w'(\vec{v},t_3)=\left[\left(\frac{\chi}{\xi(\omega_s)}\right)^2\cos\theta_{32}+\left(\frac{\delta(\omega_s)}{\xi(\omega_s)}\right)^2\right]w'(\vec{v},t_2)$$
$$-2\frac{\chi\delta(\omega_s)}{\xi(\omega_s)^2}\sin^2(\tfrac{1}{2}\theta_{32})u'(\vec{v},t_2)$$
$$-\frac{\chi}{\xi(\omega_s)}\sin\theta_{32}v'(\vec{v},t_2), \qquad \text{(A7c)}$$

where θ_{32} is given by (A2).

d. $t>t_3$. Under the same assumptions used for the $t_1<t<t_2$ region, we can proceed as in the text if some care is taken. Instead of using Eq. (45) to define $\tilde{\rho}'_{ab}(\vec{v},t,2\tau)$, we define three terms through

$$u'(\vec{v},t)-iv'(\vec{v},t)=2\{\tilde{\rho}'_{ab}(\vec{v},t,2\tau)\exp[-i\delta(\omega_0)(t-2\tau)]+\tilde{\rho}'_{ab}(\vec{v},t,t_3-t_2+t_1)\exp[-i\delta(\omega_0)(t-t_3+t_2-t_1)]$$
$$+\tilde{\rho}'_{ab}(\vec{v},t,t_3)\exp[-i\delta(\omega_0)(t-t_3)]\} \qquad \text{(A8)}$$

where each of the $\tilde{\rho}'_{ab}$ effectively is a solution of Eq. (46). The initial conditions are obtained from Eqs. (A6)–(A8) to be

$$\tilde{\rho}'_{ab}(\vec{v},t_3,2\tau)=\tfrac{1}{4}[\chi/\xi(\omega_s)]^2(1-\cos\theta_{32})\exp[-i\vec{x}(t_2,t_1)\cdot\vec{v}]\exp[y(t_2,t_1)][u'(\vec{v},t_1)+iv'(\vec{v},t_1)], \qquad \text{(A9a)}$$

$$\tilde{\rho}'_{ab}(\vec{v},t_3,t_3-t_2+t_1)=\tfrac{1}{2}\{\tfrac{1}{2}[\chi/\xi(\omega_s)]^2(1-\cos\theta_{32})+\cos\theta_{32}-i[\delta(\omega_s)/\xi(\omega_s)]\sin\theta_{32}\}$$
$$\times\exp[i\vec{x}(t_2,t_1)\cdot\vec{v}]\exp[y(t_2,t_1)][u'(\vec{v},t_1)-iv'(\vec{v},t_1)] \qquad \text{(A9b)}$$

$$\tilde{\rho}'_{ab}(\vec{v},t_3,t_3)=-\tfrac{1}{2}\{2[\chi\delta(\omega_s)/\xi(\omega_s)^2]\sin^2(\tfrac{1}{2}\theta_{32})+i[\chi/\xi(\omega_s)]\sin\theta_{32}\}w'(\vec{v},t_1). \qquad \text{(A9c)}$$

Since the velocity phase factor does not vanish at $t=2\tau$ in the second two terms in Eq. (A8), they will contribute negligibly to the echo signal at $t=2\tau$. (Their contribution will be down from that of the first term by a factor of order $e^{-ku_0\tau}<<1$.)

Thus, in the vicinity of the echo, only the lead term in the right-hand side of Eq. (A8) need be retained. Solving Eq. (46) subject to the initial condition (A9a) and calculating the corresponding u' and v' for times $t\approx 2\tau$, we find

$$u'(\vec{v},t)=\tfrac{1}{4}[\chi/\xi(\omega_s)]^2(1-\cos\theta_{32})\exp[i\vec{x}'(t,2\tau)\cdot\vec{v}]\exp[y(t,2\tau)]\exp[-i\delta(\omega_0)(t-2\tau)][u'(\vec{v},t_1)+iv'(\vec{v},t_1)]+\text{c.c.}, \qquad \text{(A10a)}$$

$$v'(\vec{v},t)=\tfrac{1}{4}i[\chi/\xi(\omega_s)](1-\cos\theta_{32})\exp[i\vec{x}'(t,2\tau)\cdot\vec{v}]\exp[y'(t,2\tau)]\exp[-i\delta(\omega_0)(t-2\tau)][u'(\vec{v},t_1)+iv'(\vec{v},t_1)]+\text{c.c.}, \qquad \text{(A10b)}$$

where x' and y' are given by Eq. (65).

Substituting in the values of $u'(\vec{v},t_1)$ and $v'(\vec{v},t_1)$ from Eq. (A1) and using Eq. (29), we finally arrive at

$$u(\vec{v},t)=\tfrac{1}{2}NW_0(\vec{v})[\chi/\xi(\omega_s)]^2(1-\cos\theta_{32})e^{y'(t,2\tau)}e^{-\Gamma_1 t}\{2[\chi\delta(\omega_s)/\xi(\omega_s)^2]\sin^2(\tfrac{1}{2}\theta_{10})\cos[\vec{x}'(t,2\tau)\cdot\vec{v}+\delta(\omega_0)(t-2\tau)]$$
$$-[\chi/\delta(\omega_s)]\sin\theta_{10}\sin[\vec{x}'(t,2\tau)\cdot\vec{v}+\delta(\omega_0)(t-2\tau)]\}, \qquad \text{(A11a)}$$

$$v(\vec{v},t)=\tfrac{1}{2}NW_0(\vec{v})[\chi/\xi(\omega_s)]^2(1-\cos\theta_{32})e^{y'(t,2\tau)}e^{-\Gamma_1 t}\{\chi/\xi(\omega_s)]\sin\theta_{10}\cos[\vec{x}'(t,2\tau)\cdot\vec{v}+\delta(\omega_0)(t-2\tau)]$$
$$+2[\chi\delta(\omega_s)/\xi(\omega_s)^2]\sin^2(\tfrac{1}{2}\theta_{10})\sin[\vec{x}'(t,2\tau)\cdot\vec{v}+\delta(\omega_0)(t-2\tau)]\}, \qquad \text{(A11b)}$$

which are valid for $t\approx 2\tau$. If needed, $w'(\vec{v},t)$ can be found by solving Eq. (43c) subject to initial condition (A7c) at $t=t_3$. The population difference $w(\vec{v},t)=w'(\vec{v},t)e^{-\Gamma_1 t}$ will be found to have "steady state" and oscillating components.

Finally, we calculate the driving term $S(t)$ for our echo field from Eq. (69b).

$$S(t)=ex_{ab}\int d^3v\,v(\vec{v},t). \qquad \text{(A12)}$$

TABLE I. Definition of some variables used in the calculation.

Variable	Definition
$\rho_{\alpha\alpha'}(\vec{R},\vec{v},t)$	$\alpha\alpha'$ density matrix element
$\tilde{\rho}_{ab}(\vec{v},t)$	$\rho_{ab}(\vec{R},\vec{v},t)\exp[-i(\vec{k}\cdot\vec{R}-\omega_L t)]$
$u(\vec{v},t)$	$\tilde{\rho}_{ab}(\vec{v},t)+\tilde{\rho}_{ba}(\vec{v},t)$
$v(\vec{v},t)$	$i[\tilde{\rho}_{ab}(\vec{v},t)-\tilde{\rho}_{ba}(\vec{v},t)]$
$w(\vec{v},t)$	$\rho_{aa}(\vec{v},t)-\rho_{bb}(\vec{v},t)$
$\vec{B}(\vec{v},t)$	$[u(\vec{v},t),v(\vec{v},t),\ w(\vec{v},t)]$
$\vec{B}'(\vec{v},t)$	$\vec{B}(\vec{v},t)\exp(\Gamma_1 t)$
$\vec{\tilde{B}}'(\vec{v},t)$	$[NW_0(\vec{v})]^{-1}\vec{B}'(\vec{v},t)$
$\tilde{\rho}'_{ab}(\vec{v},t,t')$	$\frac{1}{2}\exp[i\delta(\omega_0)(t-t')][\tilde{u}'(\vec{v},t)-i\tilde{v}'(\vec{v},t)]$
$\delta(\omega)$	$\omega-\omega_L+\vec{k}\cdot\vec{v}$
χ	$ex_{ab}E_0/\hbar$
τ	$\frac{1}{2}(t_3+t_2-t_1)$

It is not necessary for our purposes to carry out the integrations in (A12) [recall that $\xi(\omega)$, θ_{10}, and θ_{32} all depend on $\vec{v}$]. If, as in the text, the $\vec{x}'\cdot\vec{v}$ term can be dropped, then the maximum value of $S(t)$ evaluated at $t=2\tau$ gives

$$S(t=2\tau)\propto e^{y(2\tau,2\tau)}\,e^{-\Gamma_1 t}, \tag{A13}$$

which is the same result obtained in the text for our simple case. Thus, in the limit $\Gamma t\,\Delta u^2/u_0^2\ll 1$ and $\chi t_1\approx\chi(t_3-t_2)\approx 1$, the only effect of finite pulse width will be to affect the shape of the echo signal and *not* its functional dependence on the pulse separation.

APPENDIX B: THEORY OF DELAYED NUTATION

Consider a molecular velocity group that is initially excited in steady-state by a cw laser beam. It is then switched out of resonance with the optical radiation by a Stark field of pulse width τ, during which time the population of this group partially recovers. We wish to obtain an expression for the amplitude of the nutation signal, that arises when the pulse ends, as a function of the delay time τ. Our starting point is the Bloch equations (28)

$$\begin{aligned}\dot{u}&=-\delta(\omega)v-u/T_2,\\ \dot{v}&=\delta(\omega)u+\chi w-v/T_2,\\ \dot{w}&=-\chi v+(w_0-w)/T_1,\end{aligned} \tag{B1}$$

which are given here in component form. The phenomenological damping times T_2 and T_1 have been introduced where it is assumed that they dominate the relaxation behavior so that decay due to elastic collisions can be neglected. The term $w_0=\rho_{aa}-\rho_{bb}$ in the absence of an applied optical field.

For the period preceding the pulse, $t<0$, when the Stark field is off, the well known steady-state solutions[12] of (B1) apply

$$\begin{aligned}u(0)&=\frac{-\chi w_0\delta(\omega_0)}{\delta(\omega_0)^2+\chi^2T_1/T_2+1/T_2^2},\\ v(0)&=\frac{\chi w_0/T_2}{\delta(\omega_0)^2+\chi^2T_1/T_2+1/T_2^2},\\ w(0)&=w_0-\frac{\chi^2w_0T_1/T_2}{\delta(\omega_0)^2+\chi^2T_1/T_2+1/T_2^2}.\end{aligned} \tag{B2}$$

Since the velocity group under consideration is switched out of resonance by the Stark field for the pulse interval $0<t<\tau$, we may set $\chi=0$ in (B1) to obtain

$$\begin{aligned}\dot{u}&=-\delta(\omega_s)v-u/T_2,\\ \dot{v}&=\delta(\omega_s)u-v/T_2,\\ \dot{w}&=(w_0-w)/T_1.\end{aligned} \tag{B3}$$

The transverse component $(u+iv)$ gives rise to free induction decay (FID),[7] which is usually short lived compared to τ (as seen after Doppler averaging) and is of no particular interest here, whereas the longitudinal component w is crucial. The solutions to (B3) are found to be

$$u(\tau)=[u(0)\cos\delta(\omega_s)\tau-v(0)\sin\delta(\omega_s)\tau]e^{-\tau/T_2}, \tag{B4a}$$

$$v(\tau)=[v(0)\cos\delta(\omega_s)\tau+u(0)\sin\delta(\omega_s)\tau]e^{-\tau/T_2}, \tag{B4b}$$

$$w(\tau)=w_0-[w_0-w(0)]e^{-\tau/T_1}. \tag{B4c}$$

For the nutation period $t\geq\tau$ after the Stark pulse terminates we should solve (B1) again subject to the initial conditions (B4). Note that Eq. (B1) can be simplified to

$$\begin{aligned}\dot{u}&=-\delta(\omega_0)v,\\ \dot{v}&=\delta(\omega_0)u+\chi w,\\ \dot{w}&=-\chi v,\end{aligned} \tag{B5}$$

if we consider solutions of the nutation signal for sufficiently short times following the pulse so that relaxation need not be included. On the other hand, the case with damping has been reported already and could be incorporated if desired.[34] We can thus obtain, analogous to Eqs. (A7), $u(t)$, $v(t)$ and $w(t)$ in terms of $u(\tau)$, $v(\tau)$, and $w(\tau)$. However, anticipating that the terms proportional to $u(\tau)$ and $v(\tau)$ will damp rapidly due to Doppler dephasing when the field strength χ is large,[7] we keep only those terms proportional to $w(\tau)$ and find that the solution of (B5) for $t>\tau$ is

$$\begin{aligned}u(t)&=\chi[\delta(\omega_0)w(\tau)/\xi^2][\cos\xi(t-\tau)-1],\\ v(t)&=\chi[w(\tau)\sin\xi(t-\tau)]/\xi,\\ w(t)&=w(\tau)\{1+(\chi^2/\xi^2)[\cos\xi(t-\tau)-1]\},\end{aligned} \tag{B6}$$

with $\xi^2 = [\delta^2(\omega_0) + \chi^2]$ and $\delta(\omega) = (\omega - \omega_L + \vec{k} \cdot \vec{v})$.

The Doppler-averaged polarization is of a form resembling (3)

$$P = \langle e x_{ab} [u(t) \cos(\omega t - kz) + v(t) \sin(\omega t - kz)] \rangle, \tag{B7}$$

where

$$\langle u(t) \rangle \sim 0$$
$$\langle v(t) \rangle = \frac{\chi w(\tau)}{u\sqrt{\pi}} \int_{-\infty}^{\infty} e^{-(v/u)^2} \frac{\sin \xi t \, dv}{\xi} . \tag{B8}$$

and produces a change in the laser field expressed by Eq. (5).

If the active velocity group is sufficiently narrow and centered about $\vec{v}_1$, we may factor the Gaussian out of the integral and obtain

$$\langle v(t) \rangle = \chi [w(\tau)\sqrt{\pi}/ku] \, e^{-(v_1/u)^2} J_0(\chi t). \tag{B9}$$

The result (B9) exhibits the nutation oscillation behavior indicated in the zero-order Bessel function $J_0(\chi t)$ and contains as a factor the population difference $w(\tau)$ of Eq. (B4c). Thus, the initial amplitude of the delayed nutation signal, which is proportional to $\langle v(t) \rangle$, depends on the pulse width τ through $w(\tau)$ as mentioned in Sec. III B.

---

*Supported by U. S. Army Research Office.

†Sponsored in part by the U. S. Office of Naval Research under Contract No. N00014-72-C-0153.

[1]A. A. Michelson, Astrophys. J. 2, 251 (1895).

[2]H. Pauly and J. P. Toennies, in *Advances in Atomic and Molecular Physics*, edited by D. R. Bates and I. Estermann (Academic, New York, 1965), Vol. 1, p. 195; R. J. Cross, Jr., E. A. Gislason, and D. R. Herschbach, J. Chem. Phys. 45, 3582 (1966); J. H. S. Wang, D. E. Oates, A. Ben-Reuven, and S. G. Kukolich, *ibid.* 59, 5268 (1973).

[3]T. Oka, in *Advances in Atomic and Molecular Physics*, edited by D. R. Bates (Academic, New York, 1973), Vol. 9, p. 127.

[4]R. G. Brewer and R. L. Shoemaker, Phys. Rev. Lett. 27, 631 (1971).

[5]R. L. Shoemaker and R. G. Brewer, Phys. Rev. Lett. 28, 1430 (1972).

[6]R. G. Brewer and E. L. Hahn, Phys. Rev. A 8, 464 (1973).

[7]R. G. Brewer and R. L. Shoemaker, Phys. Rev. A 6, 2001 (1972).

[8]J. Schmidt, P. R. Berman, and R. G. Brewer, Phys. Rev. Lett. 31, 1103 (1973).

[9]M. Loy, Phys. Rev. Lett. 32, 814 (1974).

[10]K. L. Foster, S. Stenholm, and R. G. Brewer, Phys. Rev. A 10, 2318 (1974).

[11]E. L. Hahn, Phys. Rev. 80, 580 (1950).

[12]H. C. Torrey, Phys. Rev. 76, 1059 (1949).

[13]H. Y. Carr and E. M. Purcell, Phys. Rev. 94, 630 (1954).

[14]A. Abragam, *The Principles of Nuclear Magnetism* (Oxford U. P., London, 1961).

[15]C. P. Slichter, *Principles of Magnetic Resonance* (Harper and Row, New York, 1963).

[16]B. Herzog and E. L. Hahn, Phys. Rev. 103, 148 (1956), and references therein.

[17]R. G. Brewer, Science 178, 247 (1972).

[18]T. W. Hänsch, I. S. Shahin, and A. L. Schawlow, Phys. Rev. Lett. 27, 707 (1971).

[19]P. R. Berman and W. E. Lamb, Jr., Phys. Rev. A 2, 2435 (1972); A 4, 319 (1971); W. R. Chappell, J. Cooper, E. W. Smith, and T. Dillon, J. Stat. Phys. 3, 401 (1971); V. A. Alexseev, T. L. Andreeva, and I. I. Sobelman, Zh. Eksp. Teor. Fiz. 62, 614 (1972) [Sov. Phys.—JETP 35, 325 (1972)]; E. Ermatchenko (private communication to P. R. Berman).

[20]P. R. Berman, Phys. Rev. A 5, 927 (1972); A 6, 2157 (1972).

[21]M. Scully, M. J. Stephen and D. C. Burnham, Phys. Rev. 171, 213 (1968); J. P. Gordon, C. H. Wang, C. K. N. Patel, R. E. Slusher, and W. J. Tomlinson, Phys. Rev. 179, 294 (1969); A. B. Doktorov and A. I. Burshtein, Zh. Eksp. Teor. Fiz. 63, 784 (1972) [Sov. Phys.—JETP 36, 411 (1973)].

[22]P. R. Berman, J. Quant. Spectrosc. Radiat. Transfer 12, 1331 (1972).

[23]J. Keilson and J. E. Storer, Q. Appl. Math. 10, 243 (1952).

[24]H. C. Torrey, Phys. Rev. 104, 563 (1956).

[25]P. R. Berman, Phys. Rev. A 9, 2170 (1974).

[26]R. L. Shoemaker and R. G. Brewer (unpublished).

[27]J. M. Levy and R. G. Brewer (unpublished).

[28]J. Schmidt and R. G. Brewer (unpublished).

[29]C. Freed, IEEE J. Quantum Electron. 4, 404 (1968); 3, 203 (1967).

[30]H. Jetter, E. F. Pearson, C. L. Norris, J. C. McGurk, and W. H. Flygare, J. Chem. Phys. 59, 1796 (1973).

[31]R. G. Brewer, R. L. Shoemaker, and S. Stenholm, Phys. Rev. Lett. 33, 63 (1974); R. L. Shoemaker, S. Stenholm, and R. G. Brewer, Phys. Rev. A 10, 2037 (1974).

[32]S. Chandrasekhar, Rev. Mod. Phys. 15, 1 (1943); M. Borenstein and W. E. Lamb, Jr., Phys. Rev. A 5, 1311 (1972).

[33]For comparison note in Ref. 2 that the molecular-beam data for the total scattering cross section CH_3I with alkali halides ~5000 Å^2 (R. J. Cross, Jr. *et al.*) whereas for NH_3-NH_3 and H_2O-H_2O the value is 300–350 Å^2 (J. H. S. Wang *et al.*).

[34]F. A. Hopf, R. F. Shea, and M. O. Scully, Phys. Rev. A 7, 2105 (1973).